ACKNOWLEDGEMENTS

Fieldwork and primary compilation of the map and explanatory notes was done by a combined team from the Geological Survey of Ethiopia (GSE) consisting of staff from the Regional Geology, GeoHazard Investigation and Hydrogeology Directorates, and Czech experts from AQUATEST a.s. and the Czech Geological Survey within the framework of the Czech Official Development Assistance Program supported by the Czech Government through the Czech Development Agency. We would like to thank the SNNPR Regional Water Bureau for their hospitality, guidance and relevant data delivery. The team is grateful to the management of the Geological Survey of Ethiopia, particularly to Director General (GSE) Mr. Masresha G/Selassie and Mr. Lata Alemayehu, Head of the GeoHazard Investigation Directorate, Mr. Tadesse Alemu, Head of the Regional Geology Directorate, as well as Mr. Muhudin Abdela Head of the Groundwater Resources Assessment Directorate, for their support.

Finally, the team would like to acknowledge the untiring support of the local people who assisted the team by all means possible and facilitated the data collection and those who helped us in various different ways.

The team is also grateful to the GSE drivers, who carefully drove during the field campaign.

Žáček V., Rapprich V., Aman Y., Berhanu B., Čížek D., Dereje K., Erban V., Ezra T., Firdawok L., Habtamu M., Hroch T., Kopačková V., Málek J., Malík J., Mišurec J., Orgoň A., Pécskay Z., Šíma J., Tarekegu D., Verner K. (2014): Explanation booklet to the Set of Geoscience maps of Ethiopia at a scale 1 : 50,000: sub-sheet 0738-D3 Shashemene. 46 pgs., 5 annexes, 3 maps. Czech Geological Survey, Prague; AQUATES a.s., Prague; Geological Survey of Ethiopia, Addis Ababa.

CONTENTS

1. Summary 3

2. Introduction *(V. Rapprich, V. Žáček)* 4

3. Methods *(V. Rapprich,V. Žáček, J. Mišurec, J. Šíma, Ezra T., Z. Pécskay, V. Erban)* 5

4. Previous studies *(V. Rapprich, J. Šíma, T. Hroch, P. Kycl)* 8

5. Geomorphology 10

  5.1. Geomorphological position *(V. Rapprich)* 10

6. Geology 11

  5.1. Lithology *(V. Žáček, V. Rapprich, T. Hroch)* 11

  5.2. Tectonic settings *(K. Verner, Habtamu M.)* 20

  5.3. Geochemistry *(V. Rapprich)* 23

  5.4. Geochronology *(Z. Pécskay, V. Rapprich)* 24

  5.5. Geological evolution *(V. Rapprich)* 25

  5.6. Geological localities *(V. Žáček, V. Rapprich)* 25

7. Hydrogeology 27

  6.1. Elements of the hydrogeological system of the area *(J. Šíma)* 29

  6.2. Hydrogeological conceptual model *(J. Šíma)* 32

  6.3. Thermal water *(J. Šíma, V. Erban)* 36

  6.4. Environmental isotopes *(J. Šíma)* 38

  6.5. Water resources *(J. Šíma)* 39

8. Geological hazards 42

  7.1. Endogenous hazards *(J. Málek, V. Rapprich)* 42

  7.2. Exogenous hazards *(P. Kycl, T. Hroch, J. Malík)* 44

  7.3. Hydrological and hydrogeological hazards *(J. Šíma, T. Hroch)* 46

  7.4. Anthropogenic hazards *(V. Rapprich)* 48

9. References 49

Annexes

  Annex 1 Geochemical data

  Annex 2 Borehole inventory

  Annex 3 Dug well inventory

  Annex 4 Spring inventory

  Annex 5 Water chemistry

CD content

  Geological map

  Hydrogeological map

  Geohazards map

1. SUMMARY

Shashemene town was built on Mid Pleistocene Corbetti ignimbrites overlain by two units of younger pyroclastic deposits: yellowish phreatomagmatic tuff and Wendo Koshe pumice. The eastern part of the sub-sheet is dominated by the Wendo Genet scarp, where even older rocks crop out. In addition to silicic volcanic rocks related to the Hawasa Caldera evolution, mafic members of the Nazret Group were also documented. The Hawasa Caldera is transacted by a belt of basaltic rocks composed of scoria- and tuff-cones and basaltic lavas emitted from the cones. The rest of the Hawasa caldera is filled with polygenetic deposits of resedimented pyroclastics, as well as alluvial and lacustrine sediments.

The geological situation significantly influences the water resources. More welded ignimbrites and silicic lavas represent fissured aquifers whereas younger ignimbrites with non-welded facies and pumice fall intercalations represent combined aquifers. Unconsolidated pumiceous deposits and sediments are porous and disadvantaged by a high content of fluorine. There are numerous hot springs clustered in two areas – Shalo and Wendo Genet.

Thick accumulations of unconsolidated sediments and resedimented pyroclastics may amplify seismic effects during the next strong seismic event. The area mapped is located to the east of the Wendo Koshe Volcano, which is in a windward direction as wind blow mainly from west. A future eruption may again settle 0.5 m of pumice even in the town of Shashemene.

The steep slopes of the Weransa Ridge are prone to rock fall and toppling whereas slopes around Wendo Genet are affected by numerous ancient landslides, which could be reactivated. A serious problem in the Shashemene area is represented by non-insulated waste dumps located in highly permeable lithologies.

2. INTRODUCTION

A set of earth-science maps of the Shashemene sub-sheet 0738-D3 has been compiled through the cooperation of the Czech Geological Survey (CGS), Geological Survey of Ethiopia (GSE) and AQUATEST a.s. within the framework of the Czech-Ethiopian Development Cooperation project entitled "Capacity building in environmental geology - Mapping of geo-risks including hydrogeological conditions in Dila and Hosaina areas, Ethiopia", financially supported by the Czech Ministry of Foreign Affairs through the Czech Development Agency and by the Ethiopian Ministry of Finances and Economic Development.

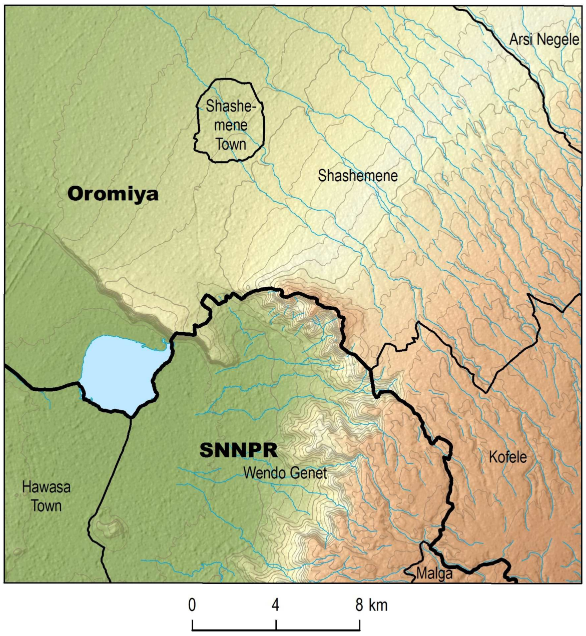

Figure 2-1. *Political subdivision of the area covered by the sub-sheet 0738-D3 Shashemene. Names of regions in bold, names of weredas (counties) in plain text.*

The Shashemene sub-sheet spreads over 763 km^2. It is located on the eastern edge of the Main Ethiopian Rift in southern Ethiopia, some 190 km south of the capital Addis Ababa by air and 250 km by road. The map sub-sheet is limited by the latitude 7°N on the south and 7.25°N on the north and by longitudes 38.5°E on the west and 38.75°E on the east. The boundary between the SNNPR and Oromiya regions crosses the area of the Shashemene sub-sheet (figure 2-1). The Shashemene sub-sheet is named after the town of Shashemene, which is an important commercial hub between southern and central Ethiopia and has more than 100,000 inhabitants. The Growth of Shashemene town and its increasing importance as well as increasing number of inhabitants requires better knowledge of the geological setting of this area giving the limits to construction work and growth of the town. The area of the Shashemene sub-sheet is divided among seven weredas. Arsi Negele, Shashemene Town, Shashemene and Kofele belong to the Oromiya region and Hawasa Town, Wendo Genet with Malga to the SNNPR region.

Shashemene lies on the Trans-African Highway 4 Cairo – Cape Town connecting this town with Addis Ababa to the north and with Hawasa and Dilla to the south, and continuing to Moyale with a border check-point to Kenya. Another asphalt road connects Shashemene with Alaba-Kulito to the west and further with Hosaina and Wolaita Soddo. Shashemene is also connected by an asphalt road with Dodola to the east. In addition to the main direct road to Hawasa, another asphalt road following the Wendo Genet scarp connects Shashemene with Wendo Genet and Hawasa.

Sinkile-Siraro hartebeest sanctuary is located to the west of the Shashemene sub-sheet area. Forests on the rift scarp to the east of the northeast tip of the sub-sheet belong to the East Langano Nature Reserve.

The highest point of the map is the Abaro peak, 2,580 m a.s.l., which is part of the Wendo Genet scarp. The lowest point is the level of Tikur Woha River which it exits the Shashemene sub-sheet area towards Lake Hawasa about 1,690 m a.s.l. Recently, the channel of the river has filled up with sediment. Most of the streams and ephemeral streams to the south of the Weransa Ridge flow into the currently sediment-filled Lake Cheleleka. Streams to the north of the Weransa Ridge and east of the Abaro - Wendo Genet Ridge flow towards Lake Shalla.

Table 1. *Used abbreviations.*

CGS	Czech Geological Survey
GSE	Geological Survey of Ethiopia
ICP-MS	Mass spectrometer with inductively coupled plasma
mg#	= 100×MgO/(MgO + FeO_{tot}) in molar values
RP	reference point
SNNPR	Southern Nations, Nationalities and Peoples Region
syn.	synonym
TIMS	Thermal ionization mass spectrometer
vol. %	volume percentages
wt. %	weight percentages
XRD	X-ray powder diffraction
XRF	X-ray fluorescence

3. METHODS

Compilation of the geological map is based on two field campaigns (figure 3-1) in 2012 and 2013 respectively, each comprising about three weeks of field work. The lithologies were described in the field, as well as the superposition or character of contact between the lithologies and their thicknesses. Approximately 150 reference points were documented during the field campaign (figure 3-2). The surface documentation has been complemented with data from 24 boreholes, 8 magnetometric profiles and 1 VES (vertical electric sounding) profile.

Figure 3-1. *Field documentation of tectonic features. Photo V. Žáček.*

A field structural analysis was undertaken in order to study the distribution, orientation and degree of development of primary structures in volcanic sequences and non-volcanic deposits, as well as lithological contacts, geological boundaries and superimposed brittle structures. The field structural data were evaluated in the programs SPHERISTAT and STEREONET using an equal projection to the lower hemisphere.

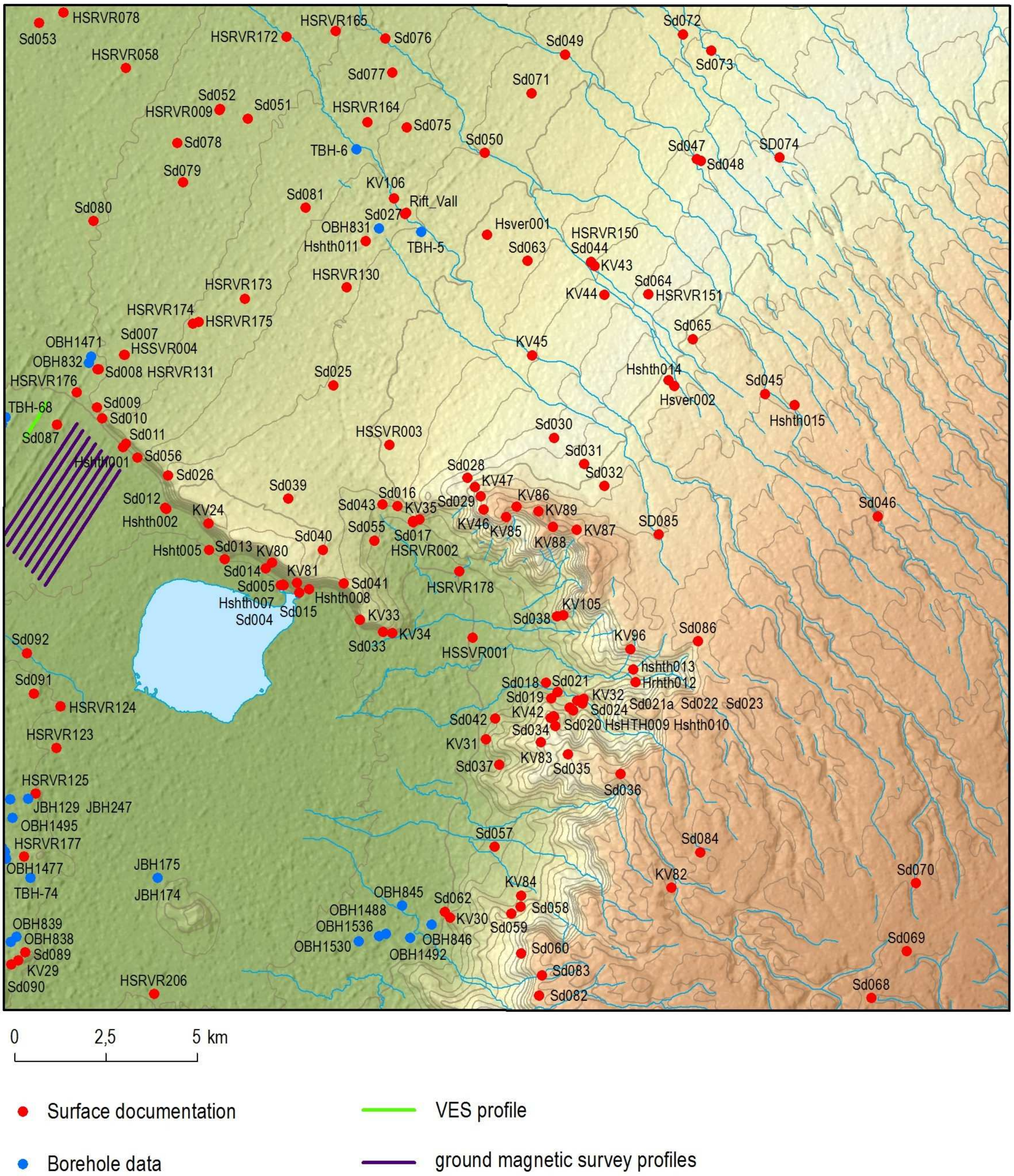

Figure 3-2. *Sketch map of reference points and location of borehole data and geophysical profiles used for construction of the maps.*

The flat area of Shalo farmland has been investigated through ground magnetic profiles using Geometrics 856 Proton Precision Magnetometer. A base station was carefully selected and established near the study area where the magnetometer was repeatedly returned after each two profiles measured to correct the daily variations of magnetic field which did not exceed 20 nT. The residual magnetic field was obtained by subtracting the regional field value (35.000 nT) from the total magnetic field values at grid cross points.

One Vertical Electrical Sounding (VES) profile was completed near the magnetic profiles. This profile consisting of 6 points was measured using the single channel American Superstring R1/IP automatic resistivity and IP system. The unit is powered by a 12V DC external battery and operates at a maximum power of either 100 or 200W depending on whether it is connected to one or two primary source batteries, respectively. The apparent resistivity values were determined automatically using the voltage difference measured between the potential electrodes and the electric current injected into ground with a consideration of the geometric factor k, which depends upon the mutual arrangement of potential and current electrodes.

In inaccessible areas, the geology was extrapolated using supporting studies of aerial photos at a scale of approximately 1 : 60,000 and satellite images. Satellite multispectral image data from Landsat TM/ETM+ and ASTER were used. As the Landsat TM/ETM+ data were obtained in several time horizons (31.1. and 9.2. 1987, 21.1. and 30.1. 1995, 5.2. and 12.2. 2000 and 16.12. 2010 and 10.1. 2011), the detection of surface changes was also available. The ASTER data were acquired on 27.1. 2006 (day-time data) and 22.11. 2006 (night-time data). Detection of terrain linear structures related to brittle tectonics and terrain morphology were interpreted using ALOS/PALSAR satellite radar data. Terrain morphology was studied mostly on the basis of a slope dependent morphometric map as well as aspect, slope and multidirectional-weighted shaded relief raster layers derived from the SRTM digital elevation model. Such an approach facilitates rapid evaluation of geomorphological forms and units and their spatial delineation. The automatically computed apparent resistivity sounding values at each station were immediately plotted on a log-log paper to check their quality and enable another observation to be taken whenever poor quality measurements were observed. VES data were interpreted in terms of layer parameters (depth and resistivity) using the IPI2WIN Version 3.1.2c software, which helps provide a the best fit of observed and calculated curves and mapinfo software.

Thin sections for petrographic classification of rocks were prepared in the GSE laboratory in Addis Ababa from twenty samples of representative rocks. Nine rock samples were taken in the area of the Shashemene sub-sheet and an additional sample in the nearby surroundings for geochemical analyses. For comparison, analyses of 4 rocks from the neighbouring Hawasa sub-sheet (Rapprich et al. 2013) were also used. All samples were crushed and pulverized in the GSE laboratory in Addis Ababa. Samples of silicic and intermediate rocks were analysed by the wet method for major oxides and by XRF and ICP-MS for trace elements in the CGS laboratories in Prague. Samples of basaltic rocks were analysed by the wet method for major oxides and by XRF for selected trace elements (Co, Cu, Ni, Pb and Zn) in the GSE laboratory in Addis Ababa. As a control, the same analyses were later carried out in the CGS laboratories in Prague using the XRF method to determine the concentrations of As, Cr, Cu, Mo, Nb, Ni, Pb, Rb, Sn, Sr, U, Y, Zn and Zr. Analytical data were processed and visualized using GCDkit software (Janoušek et al. 2006). For the analytical results see Appendix 1.

Seven rock samples (6 from the Shashemene sub-sheet area + one 1 km south of the sub-sheet area) were selected for further geochronological analyses using the K-Ar method in the ATOMKI laboratories of the Hungarian Academy of Sciences in Debrecen (Hungary). After acid digestion and 0.2M HCl dissolution of the samples, the potassium content was determined by flame photometry with a Na buffer and Li internal standard. Measurements were checked by inter-laboratory standards (Asia 1/65, LP-6, HD-B1 and GL-O). Argon was extracted from the samples by radiofrequency fusion in Mo crucibles under vacuum conditions. A ^{38}Ar-spike was added to the samples prior to gas-cleaning in Ti and SAES getters and liquid nitrogen traps, respectively. The isotope ratios of argon were measured in the static mode using a 15 cm radius magnetic sector-type mass spectrometer in Debrecen. Balogh (1985) and Odin (1982) described the methods employed in detail. Age calculations were based on constants proposed by Steiger and Jäger (1977). Results of K–Ar dating are given with 1σ errors.

The minerals present in the precipitate of the Shalo hot spring were identified using XRD in CGS laboratories in Prague.

The Sr-isotopic ratio was analyzed in two travertine samples. The travertine samples were dissolved in double distilled 6M HCl, transferred to nitrogen form and separated on Sr.Spec resin to obtain a pure

Sr fraction. This was measured using Finnigan MAT262 TIMS in the dynamic mode on a single Ta filament with addition of H_3PO_4. The quality of the measurement is checked by repeated measurement of the NBS987 standard ($^{87}Sr/^{86}Sr = 0.710243 \pm 0.000024$ (2SD), n=11).

Hydrogeology of the Shashemene sub-sheet is based on the assessment of data collected from existing reports and maps and during field work. The field water point inventory was based on a desk study, during which the relevant materials like geological and drilling reports and maps and aerial photographs were collected from the regional geology department of GSE. Important climatic and gauging station data and topographic maps were obtained from various offices. The desk study also included preliminary data interpretation and preparation of field maps using satellite images, aerial photographs and a digital elevation model (DEM) of the terrain with the geology as a background. Data assessment was mainly dedicated to data organization, processing, and interpretation in the form of maps and the text of the presented explanatory booklet. The geographic information system (GIS) ArcGis was used for compilation of the maps.

The hydrogeological map is compiled based on the methodology and standardized legend for hydrogeological maps published by the International Hydrogeological Association. The methodology classifies various lithological units based on their permeability (porous, fissured, mixed, non permeable) into aquifer/aquiclude/aquitard systems.

Classification of natural water was used to express the groundwater chemistry on the hydrochemical map. Hydrochemical types are classified based on the Meq% representation of the main cations and anions. The results of the hydrochemical study were integrated into a hydrogeological conceptual model with the aim of helping to understand the groundwater circulation within the aquifers in addition to comparing the water quality with various standards.

Hazardous phenomena were adopted from the geological map to compile the map of geological hazards. Similarly, the geological map served as a basis for the construction of the hydrogeological map, displaying the permeability properties of the lithological sequences.

4. PREVIOUS STUDIES

4.1. Geology

The Main Ethiopian Rift cannot be compared with the Afar region in terms of intensity of geological research. The area of interest has been covered by several overview geological maps of large scales. The early two-million scale map (Kazmin 1972) has been updated by Mengesha et al. (1996). The area of the Shashemene sub-sheet is also covered by the half-million geological maps compiled by Di Paola (1972), Kazmin et al. (1981) and JICA (2012). We have to express our strong criticism of the latter of the maps, as it does not respect either geological observations or morphology. A geological map at a scale of 1 : 250,000 comprising the area of Shashemene sub-sheet was compiled by Basalfew (2012). More detailed geological information can be found in the 1 : 75,000 engineering geology map (Tadesse and Zenaw 2003).

A set of geochemical and geochronological data on silicic rocks from the central part of the Main Ethiopian Rift was presented by WoldeGabriel et al. (1999). This publication deals with geochronological data previously published by WoldeGabriel et al. (1992), but unfortunately lacks the precise locations of the samples. Two K-Ar geochronological ages from the area surrounding the Shashemene sub-sheet are presented in the Report of JICA (2012).

A detailed study of the geology on the Shashemene sub-sheet concurs on the work performed on the neighbouring (to the west) Hawasa sub-sheet (Rapprich et al. 2013).

4.2. Hydrogeology

Compilation of the water resources of the Shashemene sub-sheet is based on an assessment of the data collected from existing reports and maps and during the field work.

Previous hydrogeological work at a scale of 1 : 250,000 includes the Hosaina sheet (Kefale and Šíma 2013). The area is covered by the hydrogeological map of Ethiopia at a scale of 1 : 2.000,000 published by Tesfaye (1993), and by several regional hydrogeological studies.

The first regional hydrogeological study of the Rift Valley itself was done by Tesfaye in 1982 (Hydrogeology of the Lakes Region, Ethiopia). He stated that most of the rift area is covered by volcanic rocks like basalt, ignimbrite, trachyte, rhyolite and pumiceous pyroclastic with accompanied lacustrine sediments. The extensive occurrence of the lacustrine sediments covers the rift floor. Most of these rocks have overlapping values of permeability. High fluoride concentrations in surface as well as groundwater are common.

The project entitled "Rift Valley Lakes Basin Integrated Resources Development Master Plan Study Project, June 2008, Halcrow Group Limited and Generation Integrated Rural Development Consultants, Ministry of Water Resources, The Federal Democratic Republic of Ethiopia" compiled studies of both the geology and the hydrogeological conditions of the Rift Valley Lakes basin. Representative aquifer characteristics were assessed from the point of view of water point yield and the yield for ignimbrite is 0.1 to 8.0 l/s, for basalt 2.7 to 3.0 l/s, for lacustrine sediment 1.0 to 6.6 l/s and for alluvium 1.0 to 6.0 l/s. Springs with records of both yield and temperature were also evaluated. The evaluation shows that most of the springs with high yields are from thermal spring sources. It can also be noted that thermal spring yields are highly variable (from 1.5 l/s up to 75 l/s).

An assessment of the potential of various aquifers based on the discharge of wells and springs and the major lithology by JICA (2012) showed variability of the average yield of water points from 2.8 l/s (alluvium) to 6.3 l/s (basaltic tuff). In general, highly productive water sources can be found at the foot of the escarpment based on the conclusions of the JICA (2012) study.

A detailed hydrogeological and engineering geology study of the Hawasa catchment was done by Zenaw (Tadesse and Zenaw 2003), including a point inventory and calculation of the water balance of the catchment, which was finalized in the compilation of detailed hydrogeological and engineering geology maps.

Geothermal studies consisting of geological, geochemical and geophysical investigations were carried out in the Rift Valley to determine the potential and to define feasible sites for geothermal power development (UNDP 1971).

4.3. Geological hazards

Prominent geological hazards in the Shashemene area are slope deformations and surface erosion. Geomorphological aspects of gully erosion were studied by Billi and Dramis (2003). The rate of gully development in the area was studied by Moges and Holden (2008). Controlling factors of gully development related to surface erosion were investigated by Carnicelli et al. (2009). Temesgen et al. (1999, 2001) briefly reported about slope deformation features on the Wendo Genet scarp.

5. GEOMORPHOLOGY

5.1. Geomorphological position

The studied area is located on the eastern margin of the central segment of the Main Ethiopian Rift. Two main geomorphological regions therefore join each other in the area of the Shashemene sub-sheet (figure 5-1). The western part belongs to the Rift Floor region, whereas the Eastern Highlands form the eastern part of the sub-sheet. The Eastern Highlands region with altitudes exceeding 2,000 m a.s.l. differs significantly from the rift floor area with altitudes varying between 1,700 and 1,900 m a.s.l. The map is transected by the NW–SE trending Weransa ridge with prominent tectonic escarpment (figure 5-2).

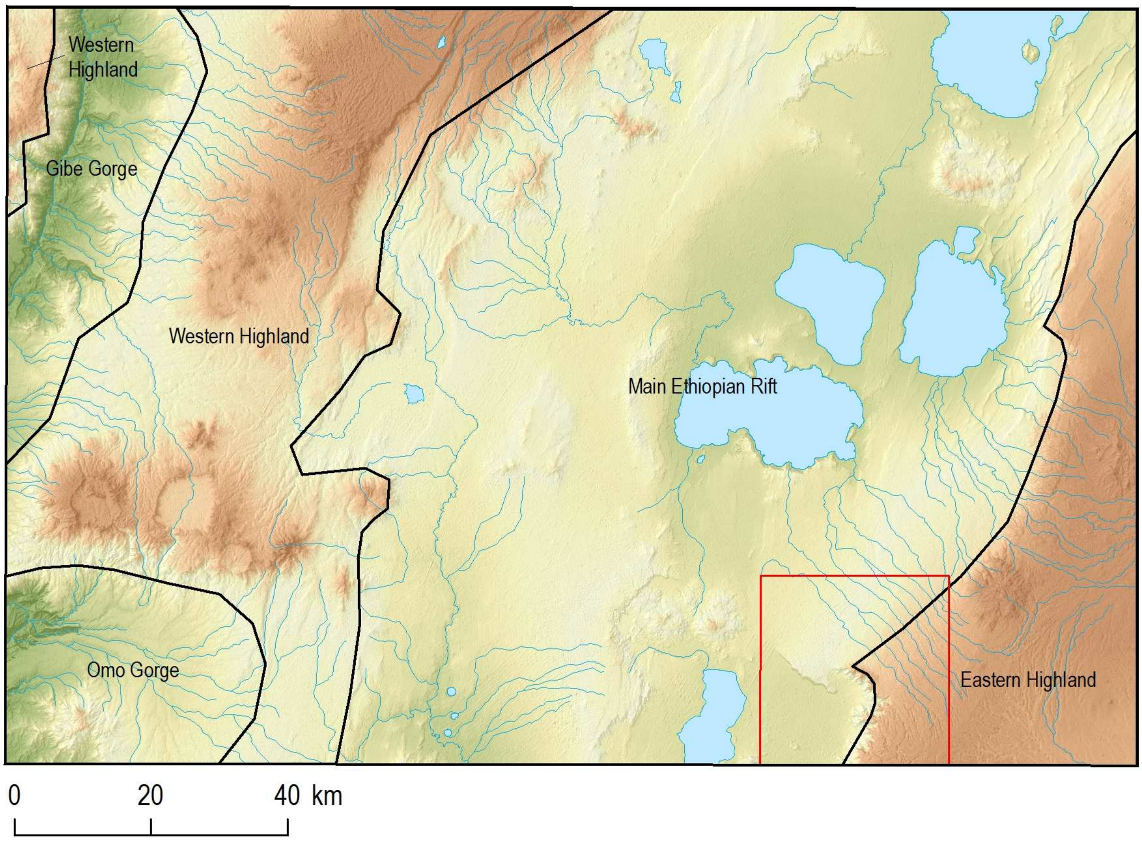

Figure 5-1. *Shashemene sub-sheet 0738-D3 (in red) within the central part of the Main Ethiopian Rift.*

Figure 5-2. *Weransa ridge escarpment above Shalo hot springs. Photo V. Žáček.*

6. GEOLOGY

The area of the Shashemene sub-sheet is located within the central part and the eastern edge of the Main Ethiopian Rift and is dominated by the eastern part of the Lower Pleistocene Hawasa caldera. Upper Miocene to Pliocene volcanic rocks of the Nazret Group composed by prevailing rhyolitic ignimbrites with intercalated basaltic units form the basement of the wider area of the Main Ethiopian Rift. The Nazret Group ignimbrites do not crop out in the mapped area and are covered by younger volcanic sequences of Lower Pleistocene to Holocene age; however basaltic units of the Nazret Group were documented. Lower Pleistocene volcanic rocks of the Dino Formation composed of rhyolitic ignimbrites, crystal-rich rhyolite, rhyodacite and trachyandesite, belonging to the volcanic activity of the Hawasa caldera are present in the central part of the mapped area, whereas in the majority of the studied territory, these rocks are also hidden below younger volcanic sequences. The subsequent volcanic sequence of the Middle Pleistocene age - Corbetti ignimbrites - is exposed in the eastern half of the map, whereas to the west it is covered by Holocene pyroclastic deposits. Basaltic lavas and pyroclastics erupted in the Hawasa basaltic belt in the south-western part of the sub-sheet most likely also during the Middle Pleistocene, and possibly lasted until the Upper Pleistocene. The youngest deposits of the Upper Pleistocene to Holocene show generally low thicknesses, mostly below 10 m but cover a significant area of the western part of the sub-sheet. The north-western corner of the sub-sheet is covered by phreatomagmatic tuff of an unclear source and pumice from the Wendo Koshe Volcano. Extensive cover of colluvial and polygenetic to lacustrine sediments is developed in the south-western corner of the sub-sheet. The dominant tectonic strikes are those of a NW-SE and NE-SW direction.

6.1. Lithology

The lithological units described in the following text are arranged generally in stratigraphic order from the oldest to youngest with descending numbering.

UPPER MIOCENE – PLIOCENE

NAZRET GROUP

19 Bale basalts: trachybasalt, trachyandesite. Trachybasaltic rock is exposed in a temporary quarry at Wetera Wendo (RP Sd042). The rock forms a sub-horizontally lying or gently inclined body or more hidden bodies (lava flows), the exposed thickness reaches about 80 m. The overlying rock is either crystal rich rhyolite or Corbetti ignimbrite; the underlying rock is not exposed but the presence of Nazret Group rhyolitic ignimbrite is supposed. We classify this rock as the Nazret Group according to the results of K-Ar geochronological analysis (10.3 ± 1.4 Ma). The mafic members of the lower (older) part of the Nazret Group are usually named as Bale or Arsi basalts, alternatively differing from Bofa basalts forming the top-most part of the Nazret Group (e.g., basalt RP Sd061 to the south of the sub-sheet with a K-Ar age of 5.51 Ma). The rock exposed in the Wetera Wendo quarry is deep-brown and displays a significantly porphyritic appearance (figure 6-1) and differs greatly from all of the other volcanic rocks in the sub-sheet area. Under the microscope the rock has porphyritic texture with prismatic euhedral phenocrysts of plagioclase up to 1 cm or longer. The rock contains about 5–10 vol. % of altered olivine, 5 vol.% of brown clinopyroxene and 2 vol.% of pale green clinopyroxene along with 1–2 vol.% of opaque mineral. The matrix has a trachytic texture with dominant prismatic acicular plagioclase and subordinate pyroxenes, olivine and opaque mineral. The pyroxenes and olivine form small phenocrysts 0.1–0.5 mm long and are also present as a part of the fine-grained matrix.

18 Nazret Group ignimbrites (only in the geological cross-section) are not outcropped in the area of the Shashemene sub-sheet and its wider vicinity but they are exposed in the rift scarps and on the rift shoulders. Welded and non-welded ignimbrites dominate this unit, with intercalations of co-ignimbrite fall deposits and minor silicic lavas. The chemical composition of the rocks representing this group corresponds to alkaline rhyolites and trachytes. The age of the Nazret group has been determined as being between 9.5 and 3 Ma (Kazmin and Seife 1978). The thickness of the Nazret Group reaches several hundred meters (400 m around Aluto Volcano: Abebe 1984; 600 m on the eastern margin of the rift WoldeGabriel et al. 1999; 500 m in the rift escarpments Basalfew 2012).

Figure 6-1. *Porphyritic texture of the trachybasalt from the Nazret Group (Wetera quarry, RP Sd042). Photo V. Žáček.*

LOWER PLEISTOCENE

DINO FORMATION-HAWASA CALDERA

17 Hawasa rhyodacite (dome) occurs as an unique small body situated in the south-western corner of the sub-sheet (RP Sd089, KV29), in the southern part of the town of Hawasa. The dome forms a conspicuous “Kike” hill being approximately 800 × 400 m in the size, and up to 100 m in height (figure 6-2), which is excavated from the western and northern side by numerous smaller or larger quarries. The quarried rock is fresh and very hard. The superficial weathered parts have probably already been excavated. The rock is whitish to yellowish fine- to medium-grained rhyodacite with a very significant, dominantly steep fluidal structure dominated by lighter and darker parallel or undulated bands (figure 6-3). The small phenocrysts (0.5–1 mm) of alkali feldspars can be observed with the naked eye. The rock has a low magnetic susceptibility ranging from 0.20 to 0.26 × 10^{-3} SI.

Figure 6-2. *Lava dome of Hawasa rhyodacites forming Kike Hill (RP Sd089). The rock showing vertical flow structures forms a conspicuous Kike hill excavated by numerous quarries. Photo V. Žáček.*

Figure 6-3. *Hand specimen of the Hawasa rhyodacite from Kike Hill (RP Sd089). Photo V. Žáček.*

16 Hawasa rhyolitic ignimbrites are the oldest rocks exposed in the area of the neighbouring Hawasa sub-sheet (Rapprich et al. 2013), but in the Shashemene sub-sheet they are only exposed in its south-western edge at Kike village. The rocks exposed on the main road represent whitish to yellowish moderately welded and relatively porous pumice flow deposits with a dominance of fine (ash) matrix over mm–cm sized pumice clasts. The sequence is stratified with a gentle dip towards the southwest. Abundant angular lithic clasts of rhyodacite up to 5 cm coming from the neighbouring dome exposed at Kike hill indicate the younger age of the pumice flow deposit. The magnetic susceptibility of the Hawassa rhyolitic ignimbrite (measured at a single locality at Kike) varies in the range of 0.13 to

0.21×10^{-3} SI. Following Rapprich et al. (2013) this unit comprises various alternating facies (welded, non-welded) of rhyolitic ignimbrites and associated fall deposits. Fragments of quartz and feldspars phenocrysts are enclosed in a groundmass of deformed glass shards and frequent fiamme. The ignimbrite of the Hawasa Caldera has been dated using the K-Ar method (JICA 2012) to 1.28 Ma using a sample taken 3 km to the south of the Hawasa and Shashemene sub-sheets (see also Rapprich et al. 2013). This age corresponds well to the ignimbrites surrounding Lake Shalla (1.35 Ma, K-Ar: JICA 2012). Ages of 1.1–1.85 Ma (K-Ar) are also given by WoldeGabriel et al. (1999). Compared to younger volcanic units, Hawasa ignimbrites are intensively jointed and faulted, also in areas where younger volcanic rocks remain un-fractured. The thickness of this unit remains unclear due to the lack of borehole data.

15 Hawasa crystal-rich rhyolite is exposed mainly along with the escarpment of the Weransa Ridge and to a lesser extent also in the area of the Wendo Genet where it occupies the base of the exposed volcanic sequence. The largest thickness of about 350 m is documented in the central part of the Weransa Ridge at Kulkuliti (RP Sd013). This rock together with the Hawasa obsidian represents the volcanic sequence (lava flows and a relic of a dome) of the former Wendo Genet Volcano of the Lower Pleistocene (Calabrian) age, as determined by K-Ar geochronology (sample Sd013: 1.18 ± 0.12 Ma). The age is nearly identical to the age of the Hawasa obsidian (see below).The underlying rock is not exposed in the localities discussed above but following regional stratigraphy a presence of the Hawasa rhyolitic ignimbrites is supposed. The overlying sequence is the Corbetti rhyolitic ignimbrite or its blocky facies exposed along the north-western part of the Weransa Escarpment. The blocks of crystal-rich rhyolite in this blocky ignimbrite clearly indicate a hiatus and unconformity between these two units. The best exposures of mostly very fresh rock are situated along the whole length of the Weransa Ridge. The rock is hard and massive, pale grey in colour (figure 6-4) and has roughly columnar jointing. The rock is weakly magnetic, its magnetic susceptibility ranges between 0.15 and 0.30×10^{-3} SI. There is no evidence of stratification but locally fluidal textures frequently appear. The fluidal texture consists of bands with variable a crystal-size distribution (figure 6-5). Numerous conspicuous phenocrysts of quartz 0.5–5 mm long are enclosed in a grey fine-grained matrix. The quartz phenocrysts frequently display a false cleavage and look like feldspars and the rock has nearly trachytic appearance. Under the microscope the rock has a porphyritic texture, the phenocrysts are subhedral to euhedral, mostly 1–3 mm long, and the minerals are mostly randomly oriented but locally their orientation respects the fluidal texture. The matrix is mostly fine-grained and completely crystallized, it is formed by a mosaic of lath-shaped feldspars, grains of quartz, relatively abundant bluish-greenish strongly pleochroic amphibole and scarcer probable brown biotite, along with unidentified tiny semi-opaque to opaque inclusions. The amphibole either forms a subhedral to anhedral fragment of phenocrysts or is patchy, skeletal or forms symplectitic intergrowths with the matrix minerals. Its amount in the rock varies between 5 and 15 vol. %. Some domains originally had a glassy groundmass, as documented by the presence of spherulites (texture resulting from the recrystallization of glass).

Figure 6-4. *Outcrop of the massive Hawasa crystal-rich rhyolite displays a locally significant fluidal structure. Southern edge of the Weransa Ridge next to Shalo hot springs (RP Sd015). Photo V. Žáček.*

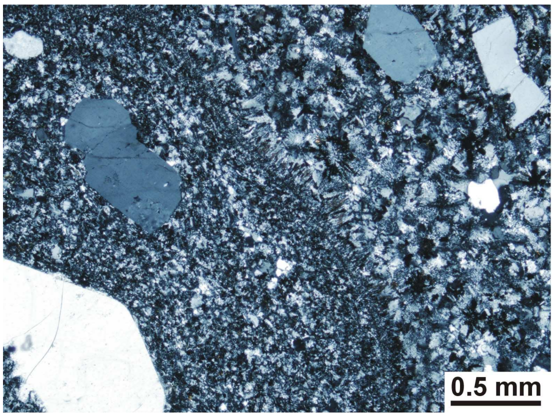

Figure 6-5. *Microphotograph of two distinct bands in the Hawasa rhyolite (RP Sd013). The originally glassy groundmass is recrystallized to spherulites in the right band. Cross-polarized light, photo V. Rapprich.*

14 Hawasa obsidian is well exposed in two big temporary quarries by the road from Shashemene to Wendo Genet (RP HSRVR002, Sd016, Sd017). It forms a lenticular body – former Wendo Genet Volcano or dome, with a maximum thickness exceeding 600 m. The Corbetti ignimbrite clearly overlies, with a certain unconformity, the obsidian body whereas the underlying unit is not exposed but the presence of Hawasa ignimbrites is assumed. The lithology is highly variable; whitish yellowish significantly fluidal rhyolitic lava flows, alternating with steeply dipping layers of rhyolitic breccias (autoclastic breccia in the carapace facies of the lava dome – figure 6-6). The lava flows contain obsidian in various stages of recrystallization: from fresh black glassy obsidian, over obsidian with white spherules (up to 3 cm in diameter) to nearly completely recrystallized glass with a spherulitic texture. Black obsidian is preserved in patches, layers or lenticular domains several dm to several m long. The whole sequence is intensively faulted and brecciated, and hydrothermally altered zones occur locally. Sample Sd017 (dated by K-Ar, see below) has a microspherulitic texture and contains approximately 20 vol. % of glass with scarce anhedral quartz phenocrysts and tiny patchy semiopaque brown mineral. Magnetic susceptibility of the rock is surprisingly elevated (possibly due to oxidation) but it principally corresponds to high lithological variability, ranging between 0.30 and 5.5×10^{-3} SI, but the majority of measurements fall within the interval $1.0–3.0 \times 10^{-3}$ SI. The determined K-Ar of the Sd017 sample (from the big/lower quarry) yielded an age of 1.02 ± 0.14 Ma, documenting the Lower Pleistocene Calabrian age and fits well with the age of the crystal-rich rhyolite. These new radiometric data document well the middle Calabrian age of the magmatic activity of the former Wendo Genet Volcano as the latest period of the Hawasa Caldera activity.

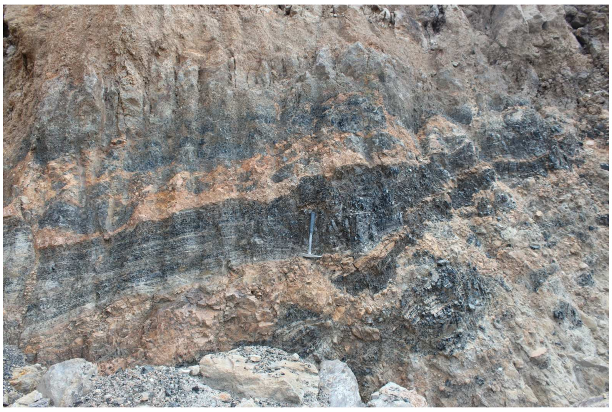

Figure 6-6. *Layers of coherent obsidian lava alternating with autoclastic facies (Herebate quarry, RP Sd016). Photo V. Žáček.*

Figure 6-7. *Blocky facie of the Corbetti ignimbrite exposed at the NW edge of the Weransa Ridge (RP Sd007). Photo V. Žáček.*

MIDDLE PLEISTOCENE

CORBETTI CALDERA

13 Corbetti blocky rhyolitic ignimbrites are exposed exclusively in the north-eastern part of the Weransa Ridge escarpment (RP Sd007). Their continuation to the northeast or other possible occurrences is obscured by younger volcanic deposits. The contact with the underlying crystal-rich rhyolite is observed well with clear unconformity, the thickness of the exposed part of the Corbetti rhyolitic ignimbrite-blocky facies reaches about 100 m. The rock is a stratified or layered solidified pyroclastic flow deposit, with the thickness of individual flow units from several dm to several m. The matrix dominates over the supported clasts and blocks (figure 6-7), and the development of degasation is common. The bedding is subhorizontal with a gentle dip towards west or southwest. The rock is composed of a brownish fine-to medium-grained matrix with abundant subangular to angular blocks of underlying crystal-rich rhyolite. The size of clasts is commonly 5–20 cm, rarely reaching 1 m. The magnetic susceptibility of the rocks varies between $0.40–0.50 \times 10^{-3}$ SI. The rock is considered as the basal facies of the Corbetti ignimbrite, the probable age, based on analogy and the stratigraphy of the recently dated Corbetti ignimbrite can correspond to ~700 ka.

12 Corbetti rhyolitic ignimbrite represents the complex of volcanic deposits of rhyolitic composition which dominates in the surface geology of the eastern half of the sub-sheet (RP Sd048, Sd045, Sd046, Sd086 and others) although it is frequently covered by thin accumulations of Wendo Koshe fall deposits. The Corbetti Caldera is situated out of the sub-sheet in the north-western part of its ancestor, the Hawasa Caldera (Rapprich et al. 2013). Stratigraphic relations indicate that the complex can reach a thickness of about 700 m. As the petrography and composition of Middle Pleistocene Corbetti ignimbrites resemble the characteristics of the underlying Lower Pleistocene Hawasa ignimbrites, the boundary between these two can be unclear in the Hawasa area (Rapprich et al. 2013). However, in the Wendo genet and Weransa Ridge areas of the sub-sheet, these two units are intercalated or separated by lavas of the former Wendo Genet volcano. The ignimbrite sequence consists of welded (figure 6-8) and non-welded (RP Sd020, figure 6-9) facies alternating a number of times. The welded facies are formed by greyish to pinkish typical stratified ignimbrite with more or less conspicuous black fiamme (figure 6-8), mm–cm sized lithics of silicic rocks, abundant subhedral fragments of the phenocrysts (crystaloclasts) of quartz in the size of several mm and less abundant and smaller crystaloclasts of green amphibole along with accessory semi-opaque brownish mineral. Non-welded facies are yellowish or greyish tuffs representing pumice-ash flow deposits and co-ignimbritic ash-fall deposits. The thickness of individual facies can vary significantly from a few to tens of metres. The ignimbrite from the Corbetti Caldera sampled at Alaba-Kulito (ca 20 km to the west of the Hawasa sub-sheet) was dated using the K-Ar method (JICA 2012) to 0.19 Ma. Three new K-Ar geochronological results from the Shashemene sub-sheet confirmed the age of the previous dating. Sample Sd048, from a small quarry at Jigesa, 8 km ENE of Shashemene yielded an age of 0.20 (± 0.14) Ma. The second dated ignimbrite, a sample from a small local quarry near a road on the mountain ridge, 3 km to the southeast of Wendo Genet hot spring, yielded 0.67 (± 0.13) Ma. Published and recent data hence indicate a polyphase evolution of the Corbetti Caldera in a time span of 700 to 200 ka with a single age of 0.98 (± 0.26) for the sample Sd067.

Figure 6-8. *Hand specimen of welded facies of the Corbetti ignimbrite (RP Sd048). Photo V. Žáček.*

Figure 6-9. *Non-welded facies of the Corbetti ignimbrite overlying paleo-soils (RP Sd020). Photo V. Žáček.*

UPPER PLEISTOCENE – HOLOCENE

POST-CALDERA MAFIC VOLCANISM

11 Hawasa basalt forms a ridge (RP HSRVR123, HSRVR124, SD091) transecting the Hawasa Caldera in an N-S direction. The ridge subdivides the caldera into the western part with Lake Hawasa on the Hawasa sub-sheet and the eastern part with the former Lake Cheleleka on the studied sub-sheet. Lavas of the Hawasa basaltic ridge were emitted from several scoria- and tuff-cones arranged along the ridge. Most of the cones are located to the south of the Tikur Woha River, but one tuff-cone has been documented further north on the Hawasa sub-sheet (Rapprich et al. 2013). Lava flow most likely emitted from this tuff-cone has been detected by a VES profile embedded within the polygenetic sediments and covered by younger pyroclastic deposits (figure 6-10). The presence of basaltic lavas beneath younger pyroclastic deposits and embedded within the polygenetic sediments was also detected by a ground magnetic survey in the Shalo farmland to the north of Tikur Woha River and to the east of the Shashemene – Hawasa road (figure 6-11). The gentle anomalies with an amplitude of about 250 nT in the southwestern and northwestern parts of the investigated area most likely represent buried basaltic lavas of a small thickness, whereas the prominent anomaly to the east reaching some 500 nT should represent a buried conduit probably of an eroded scoria/tuff-cone. The thickness of the basaltic lava flows most probably does not exceed several tens of metres. The underlying rocks are either rhyolitic ignimbrites of the Dino Formation of the Lower Pleistocene age or lower parts of polygenetic sediments of lakes Hawasa and Cheleleka. The lavas and coherent feeders of pyroclastic cones (RP HSRVR125, HSRVR177) consist of basaltic rock with relatively large phenocrysts of olivine (up to 1 mm, mostly discomposed) and plagioclase (up to 2 mm) and frequently small phenocrysts of clinopyroxene (not exceeding 0.3 mm) enclosed in a matrix of plagioclase, clinopyroxene, olivine and magnetite. The basalts are slightly alkaline and are plotted on the TAS diagram at the boundary with the basanite (see the Geochemistry chapter).

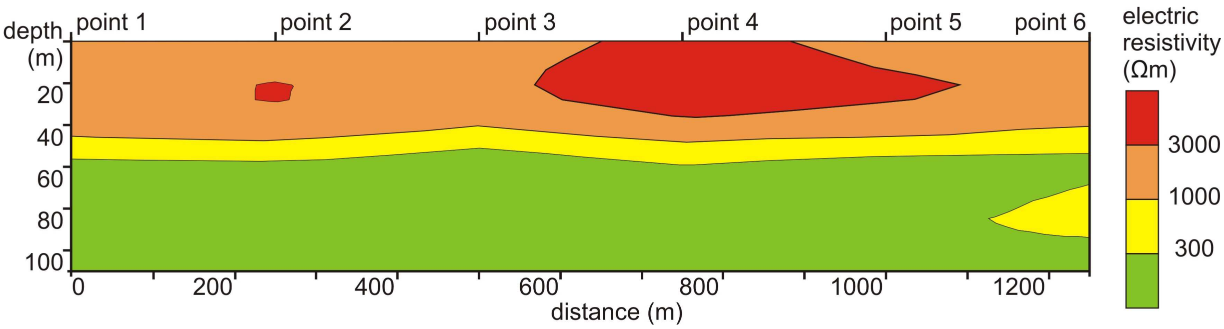

Figure 6-10. *VES (vertical electric sounding – see figure 3-2 for location) profile discovering basaltic lava (extremely high resistivity) embedded in the polygenetic infill of the Hawasa caldera. Measured by Ezra T.*

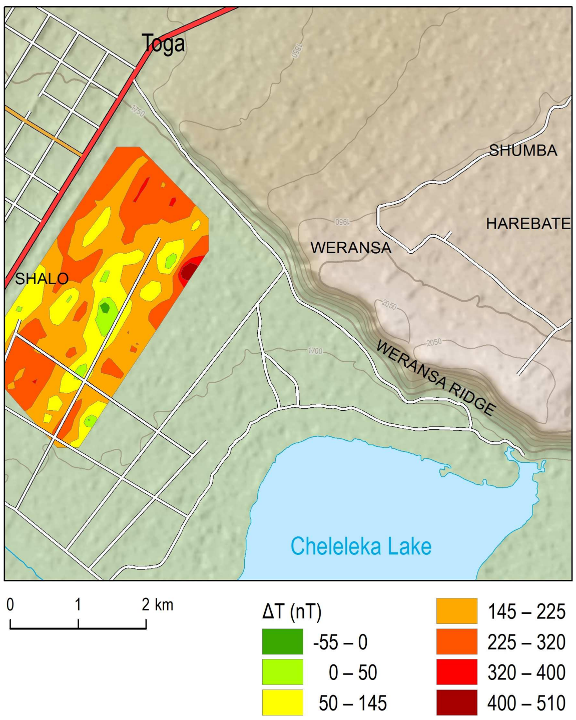

Figure 6-11. *Sketch map of magnetic field variability in the Shalo farm area. Measured by Ezra T.*

Figure 6-12. *Ilala (syn. Ilanta) tuff-cone in the marshy plain south of Lake Cheleleka. Photo V. Rapprich.*

Figure 6-13. *Fragment of basaltic scoria from the cone on Weransa ridge (RP Sd056). Photo V. Žáček.*

10 Basaltic lapilli-stone (tuff cone) forms the Ilala or Ilanta volcanic cone (figure 6-12) with a well-preserved crater structure in the southern part of the former Lake Cheleleka. The cone forms an island with a diameter of about 2 km surrounded by a swamp of the former Lake Cheleleka. The extent of the lapilli-stones is limited to the size of tuff cones and their thickness to the height of these cones. The lapilli-stones are poorly-sorted clast-supported and dominated by massive non-vesicular basaltic clasts with a prevailing grain-size of 1 cm, but larger clasts (up to 20 cm), often with xenolith in the core, may also occur. These pyroclastic deposits were produced by phreatomagmatic (Surtseyan) eruptions in marshy or shallow-lake environments. As the Ilala cone is not accessible most of the year, the detailed description is based on correlation with observed tuff-cones in the area of the Hawasa sub-sheet (Rapprich et al. 2013).

9 Basaltic scoria (scoria cone) can be found forming three cones situated on the Hawasa basaltic ridge in the south-western part of the sub-sheet (RP HSRVR125 = geological locality 1, HSRVR177). An additional small cone is situated in the north-eastern part of the Weransa scarp (RP Sd056). The last occurrence can be found near the road from Shashemene to Alaba-Kulito in the north-western edge of the sub-sheet. The occurrences are small but all are well exposed by temporary quarries. The scoria is poorly sorted and clast-supported, dominated by fragments of scoria predominantly 1–20 cm in diameter (figure 6-13), frequently with large bombs. The bombs are flattened in the crater facies, whereas in the wall facies spindle shaped bombs can be found. The prevailing scoria is associated with minor basaltic lava flows up to several m thick. Such deposits correspond to Strombolian style eruptions. The magnetic susceptibility is highly variable depending on the porosity of the rock; the porous scoria has a magnetic susceptibility of about 10×10^{-3} SI, the coherent massive lavas display values much higher, up to 68×10^{-3} SI. Similarly to the lapilli-stones, the extent of the scoria deposits does not exceed the size of the scoria cones and their thickness is equivalent to the height of the cones. The age is estimated as being Middle Pleistocene, but possibly lasting until Late Pleistocene. No current fumarolic activity has been documented associated with the scoria cones.

Silicic Pyroclastic Deposits

8 Yellowish phreatomagmatic tuff belongs to the youngest volcanic deposits most probably of the Upper Pleistocene age. This tuff covers nearly the entire area of the sub-sheet, except of the southern part and stream gorges where the tuff was washed out by erosion. Although the majority of the extent of this tuff is hidden below the deposits of the youngest Wendo Koshe pumice fall, its presence is well documented in numerous mudpits and several large sandpits dispersed throughout the territory (RP HSRVR009: figure 6-14, HSRVR175, Sd040, Sd063, and others).

Figure 6-14. *Sandpit in phreatomagmatic tuff with > 6 m thickness overlain by Wendo Koshe pumice (RP Sd009). Photo V. Žáček.*

Figure 6-15. *Roof of the sellers at Shashemene exposing an ash-flow deposit overlain by an ash-cloud surge and ash-fall deposits (RP HSRVR175). Photo V. Rapprich.*

The thickness of the deposits systematically decreases from the west (WNW) to the east (ENE). The maximum thickness exceeding 6 m was documented in a sandpit in the north-western quarter of the sub-sheet (RP HSRVR009, geological locality 3). The thickness of 3–4 m is supposed within Shashemene town, whereas in the Sole quarry (RP KV44 = geological locality 5) the thickness does not exceed 2 m. Towards the east and southeast, the thickness of the phreatomagmatic tuff decreases further. Strong lateritization of the phreatomagmatic tuff as well as the underlying welded Corbetti rhyolitic ignimbrite in the eastern part of the sub-sheet obscures the boundary between these two lithological units. Where the boundary remains clear, the surface of the Corbetti ignimbrite flow is irregular with pockets filled with the phreatomagmatic tuff. The depositional processes of the yellowish phreatomagmatic tuff can be best studied in cellars excavated during last 30 years near Shashemene by a local inhabitant (RP HSRVR175, geological locality 2, figure 6-15). The tuff is loose and poorly solidified, but the textures allow interpretation of depositional processes. The exposed deposit (with total thicknes of about 6 m) is dominated by two ca 2 m thick units of matrix-supported yellowish to brownish tuff with small clasts of pumice or vitreous rhyolite reaching 10 cm, but mostly much smaller. The lower matrix supported unit overlays paleo-soil developed upon Corbetti ignimbrite and contains in its basal part pieces of this paleo-soil up to 30 cm in diameter. We interpret these matrix supported units as ash-flow deposits. These two main units are separated by a sequence (1–1.5 m thick in total) of well-sorted massive ash layers with abundant accretionary lapilli (ash-fall deposits) alternating with diagonally bedded layers (ash-cloud surge deposits). The horizon of the fossil soil (paleo-soil) with a thickness of 30–80 cm and a deep brown colour is developed on the top of the tuff sequence, mostly covered by a layer of the youngest pumice fall originating form the Wendo Koshe Volcano. It remains unclear whether this tuff originated from an ancestor eruption of the Wendo Koshe Volcano or from the Fike Volcano between the lakes Shalla and Abijata, which is built of yellowish pyroclastic deposits apparently from phreatomagmatic eruptions.

NON-VOLCANIC DEPOSITS

7 Laterite is present in the eastern part of the Shashemene sub-sheet as a weathering product of poorly consolidated pyroclastic deposits represented by yellowish phreatomagmatic tuff and poorly welded facies of the Corbetti ignimbrite with associated co-ignimbritic ash-fall deposits. The thickness of the lateritization commonly exceeds 10 m. The laterites have reddish brown colour and when wet become plastic.

6 Polygenetic sediments (resedimented pyroclastics, alluvial sediments, lacustrine sediments) fill the basin of the former Lake Cheleleka in the south-western corner of the sub-sheet. The lake originally occupied the eastern part of the Hawasa Caldera separated from Lake Hawasa to the west by the Hawasa basaltic belt. Recently we speak about the former lake, because the whole basin, including its northern part which is marked in the topographic map as Lake Cheleleka, is completely filled by sediment, and its remnants are represented by a network of irregular channels surrounded by an extensive swamp. The sediments are characterized by alterations of beds and successions with various origins and lithology. The character of the sediments is a result of tectonic, volcanic and exogenous processes and fluctuations of water levels in the lake. They represent a mixture of re-sedimented loose pumice or mixtures with a low portion of silt, sand or soil. Greyish to black mud rich in organic compounds is locally developed. Locally clasts of weathered ignimbrites, and tuffs occur.

HOLOCENE

5 Wendo Koshe pumice fall and minor flow deposits (>30 cm) cover a large area in the north-western quarter of the map. We present the extent of deposits with thickness exceeding 0.3 m on the geological map; however thicknesses of 2, 1.5, 1.0, 0.5, 0.3 and 0.1 m are also depicted as individual isopachs. The fall deposits were undoubtedly produced during the last violent explosive event of the Wendo Koshe Volcano situated on the neighbouring Hawasa sub-sheet (Rapprich et al. 2013). The underlying rock is yellowish phreatomagmatic tuff, typically topped by a well-developed horizon of paleosoil. The pumice deposits are whitish to greyish, well-sorted and clast-supported. They are topped by a horizon of relatively poorly developed recent soil. The thickness of the deposits increases continuously from ESE to WNW, the maximum thickness exceeding 2 m was recorded in the NW part of the map and around the Shashemene-Hawasa road (RP HSRVR131, figure 6-16). The maximum size of the clasts correlates well with the thickness of the deposits and with the distance from the Wendo Koshe Volcano; the following data express the thickness of the pumice deposits in metres versus the approximate maximum size of the clasts: 2.0 m / 6 cm, 1.5 m / 5 cm, 1.0 m / 4 cm, 0.5 m / 3 cm, 0.3 m / 1.5 cm, 0.2 m / 1 cm, 0.1 m / 0.5 cm. The poorly developed recent soil upon the pumice and the fact that the pumice fall covers the colluvial deposits below Weransa Ridge indicate a very young, most probably Holocene age, however the exact age of this eruption yet to be determined.

NON-VOLCANIC DEPOSITS

4 Colluvial sediments occur exclusively on the western slope of the Wendo Genet scarp (RP Sd018 and Sd023) and rimming the escarpment of the Weransa Ridge. Most voluminous deposits with a supposed thickness of several tens of metres situated at the steep slopes of the Wendo Genet were produced by large-scale but mostly fossil rock-slides. The alternation of solid ignimbrite layers with poorly solidifies tuffs and pumice deposits exposed in the steep scarps create favourable conditions for rock-falls and landslides. The ignimbrites, associated poorly solidified pyroclastics and brownish soils derived from laterite form the dominant lithology of the colluvial sediments. The uppermost part of these deposits is formed by unsorted clast-supported deposits (figure 6-17) with a prevalence of blocks reaching up to several metres in diameter but highly variable in the size. Down the slope, the character of the deposits changes to a prevailing structure of unsorted matrix supported deposits with blocks and boulders of variable size up to 2 m (figure 6-18). A transition to fine-grained polygenetic colluvial to alluvial sediments forming wide flat fans can be seen in the lowermost part of the colluvial deposits.

Figure 6-16. *More than 2 m thick deposit of Wendo Koshe pumice-fall near the road Shashemene-Hawasa (RP HSRVR131). Photo V. Rapprich.*

Figure 6-17. *Blocky colluvia cemented by travertine exposed along the Werka Stream in the vicinity of the Wendo Genet hot springs (RP Sd023). Photo V. Žáček.*

Figure 6-18. *Colluvial deposits with blocks of rhyolites and ignimbrites within re-sedimented brown soil (Wendo Genet area, RP Sd018). Photo V. Žáček.*

3 Fine-grained polygenetic colluvial to alluvial sediments form mostly 3–4 km wide rim of the eastern shore of the former Lake Cheleleka in the central-southern part of the sub-sheet. They occur as very flat and wide alluvial fans passing more or less continuously to polygenetic sediments forming the fill of the basin of the former Lake Cheleleka to the west. No sharp boundary can be seen with the colluvial sediments in the Wendo Genet area to the east. Alluvial sediments are formed by re-sedimented soil and fine- to medium-grained sands with a high portion of weathered volcanic rocks and volcaniclastics. Small angular clasts of pumice or silicic volcanic rocks are common within these sediments. The sediments accumulate due to a deceleration of flow at lower gradients, their formation and creation is related mainly to erosion and re-sedimentation of colluvial sediments during the rainy season.

2 Fluvial sediments are poorly developed on the Shashemene sub-sheet because of a lack of fluvial systems in the lowlands (Cheleleka lake basin), while the small rivers and brooks in the highlands in the eastern and north-eastern part of the sub-sheet have an erosional character. The limited occurrence of fluvial sediments consisting of silty and muddy unconsolidated deposits is related to a drainage channel connecting Lake Hawasa with the former Lake Cheleleka (Tikur Woha) in the south-western part of the sub-sheet. The fluvial fill of the small rivers within the area of polygenetic colluvial to alluvial sediments is similar but in the upper parts of the flow in the valleys of the Wendo Genet area sandy material gravel or even boulders prevail.

1 Anthropogenic deposits are represented in the area of the Shashemene sub-sheet by waste dumps around the town of Shashemene. One of these dumps is located on the south-eastern edge of the city in an abandoned sand-pit. The second one is located some 4 km to the west of Shashemene. The mixed communal waste is deposited in a thickness reaching 6–10 m without any insulation on permeable unconsolidated pyroclastic deposits, represented mostly by pumice. Deposition of such material, frequently containing spent chemical bottles and containers, on highly permeable rocks without any insulation (plastic foil) represents the most serious risk to human health and the environment in the area of Shashemene.

Travertine occurrences (not polygons, only point marks on the map) are associated with several calcium-carbonate hot springs in the area. The travertine cements the colluvial deposits (RP Sd023, figure 6-17) or forms small travertine moulds (RP HSRVR178, figure 6-19). Periodic precipitation of carbonate causes the bedded structure of the carbonate. The origin of the travertines is discussed in the chapter Hydrogeology.

Figure 6-19. *Travertine at the hot spring north of Wesha (RP HSRCR178). Photo V. Rapprich.*

6.2. Tectonic setting

The geological map at a scale of 1 : 50,000 Shashemene sub-sheet is situated on the eastern margin of the NNE–SSW to NE–SW trending Main Ethiopian Rift which belongs to the regional East African Rift System (e.g., Hayward and Ebinger 1996; Bonini et al. 2005). This rift structure accommodates the active extension between the Nubian and Somalian plates since the Late Miocene (e.g., Ebinger 2005). This area underwent a typical evolution of continental rifting, from fault-dominated rift morphology in the early stages of the continental extension (transtension) toward magma-dominated extension during break-up (e.g., Agostini et al. 2011; Accocella 2013). Minor Holocene re-sedimented pyroclastic deposits with intercalations of lacustrine sediments dominate the southern part of the map sheet. In other lithologies such as effusive rocks and rhyolithes with cognate pyroclastics, a set of primary volcanic fabrics (e.g., flow-banding and flow-foliation) was observed. The origin of these structures is related to a flow-stretching of viscous silicic lava or hot fragmentary density flows. All of these primary fabrics were affected by brittle rift-related deformation.

PRIMARY AND DUCTILE STRUCTURES

The rhyolites reveal flow-banding structures defined by the planar preferred orientation of rock-forming minerals or domains with variable amounts of micro-vesicles or micro-crysts (figures 6-20 and 6-21). In the Wendo Genet area (central part of the map sheet) their orientation is mostly subhorizontal (figure 6-22 left; maxima in centre of the diagram). However along the ~ NNE–SSW regional faults the original flow-banding was folded into asymmetric folds. Corresponding fold limbs dip under various angles to the ~ ESE or WNW (figure 6-22 left). Corresponding fold axes and associated stretching lineation plunge under low angles towards the ~ NNE or SSW (figure 6-22 left).

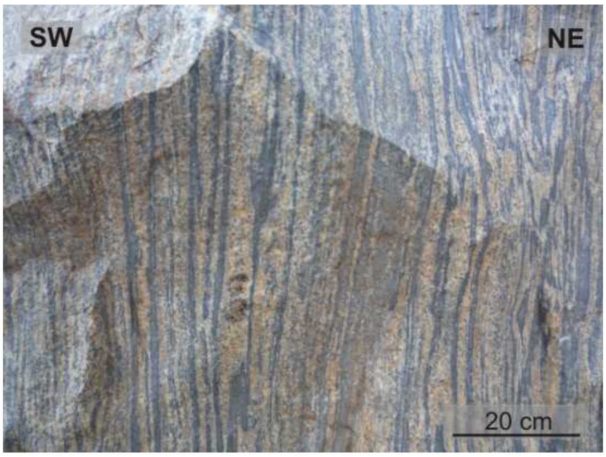

Figure 6-20. *Original steeply dipping flow-banding in rhyolites (active quarry in Hawasa, RP KV29). Photo K. Verner.*

Figure 6-21. *Asymmetric folds of flow-banding related to ~ NNE–SSW regional faults (Ebicha). Photo K. Verner.*

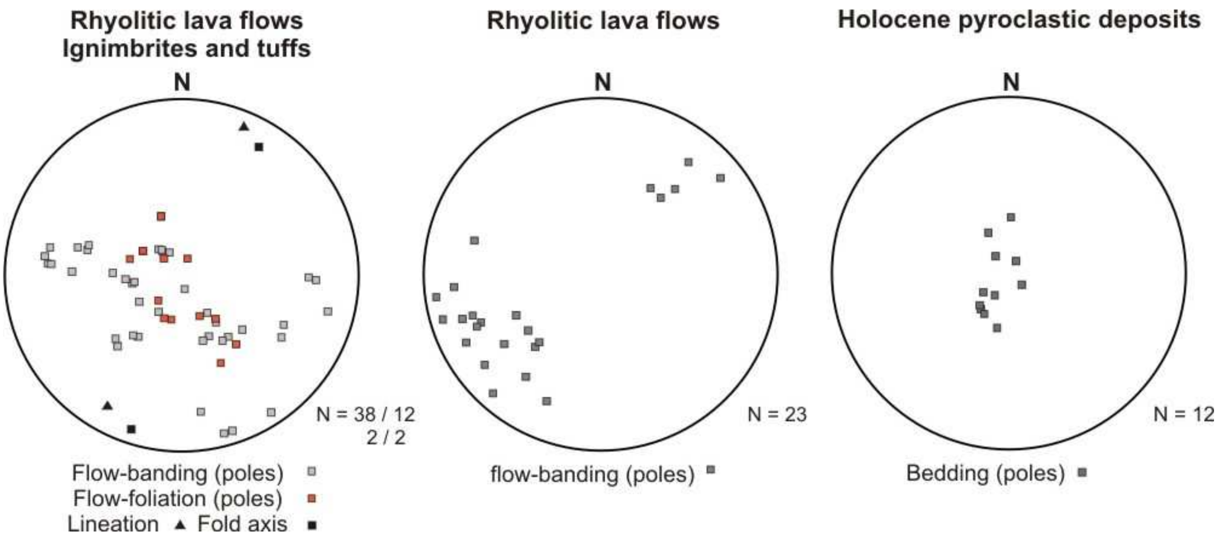

Figure 6-22. *Orientation diagrams of primary and ductile structures: (left) fabrics in rhyolites and ignimbrites; (centre) fabrics in rhyolites (active quarry in Awasa); (right) sedimentary bedding in Holocene deposits (poles). Equal projection to the lower hemisphere.*

The axial planes have a steep to moderate orientation dipping to the ~ ESE (figure 6-22 left). On the locality of active quarry of Hawasa (southern part of the map sheet) flow-banding has ~ SW or ~ NE steeply dipping orientation (figure 6-22 centre). Ignimbrites display well-developed flow-foliation dipping predominantly at low angles to the ~ SSE, N or NW (figure 6-22 left). The bands of ~

centimetre scale often contain elongated mineral grains and lithic fragments or stretched and welded pumice fragments. The Holocene deposits show sedimentary bedding in a subhorizontal orientation or gently dipping to the south (figure 6-22 right).

BRITTLE STRUCTURES

Across the map sheet normal and strike-slip faults or fault zones were identified (figure 6-23). The faults dip steeply to ~ ESE (E) or WNW (W) bearing well developed steeply plunging slickensides (figures 6-24 and 6-25 left). Observed slickenside asymmetry reveals normal movement in the direction of the lineation. These faults are mostly parallel to the main axis of the East African Rift System and morphological escarpments. Subordinate sets of faults predominantly have a (figure 6-25 centre): (a) ~ WNW–ESE trend mainly bearing dextral strike-slip kinematic indicators, (b) ~ NE–SW trend also showing a dextral strike-slip component of movement and (c) ~ N–S trend with indicators of sinistral kinematics. At several localities across the mapped area the strike-slip faults appear to be older than normal regional faults. Extensional joints occur in four sets across all of the lithological units. The main trends of their orientation are mostly parallel to the regional faults, predominantly ~ NNE–SSW, NNW–ESE, WSW–ENE and also in some cases WNW–ESE (figure 6-25, on the right).

Figure 6-23. *Regional NNE–SSW trending fault with normal component of movement (Wendo Genet, RP KV35). Photo K. Verner.*

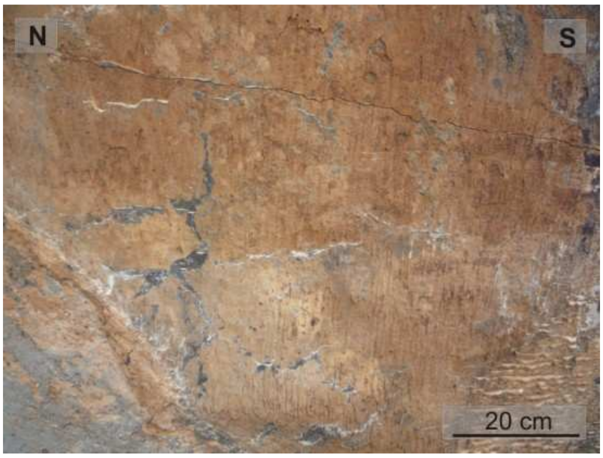

Figure 6-24. *Normal fault bearing well developed steeply plunging slickensides (Wetera, RP KV31). Photo K. Verner.*

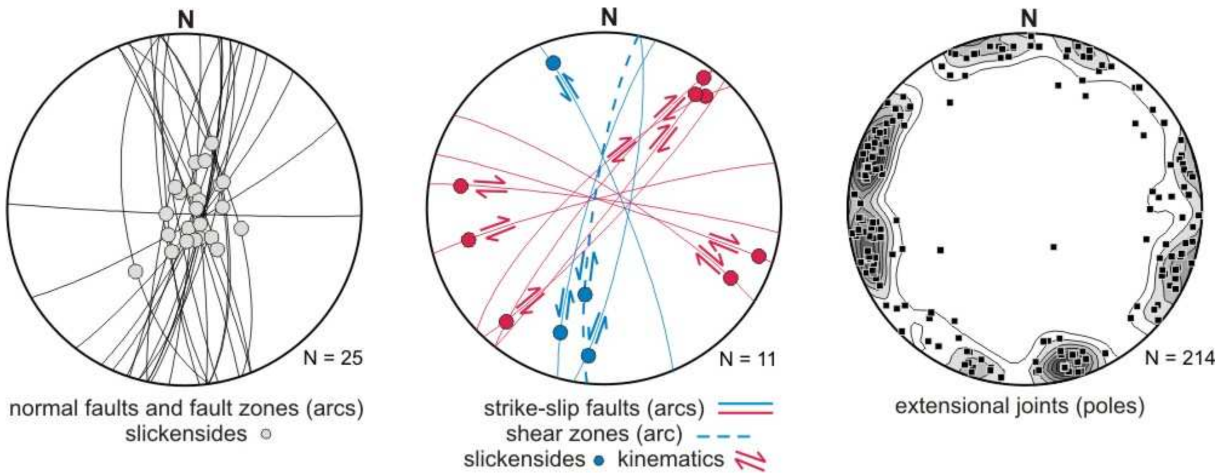

Figure 6-25. *Orientation diagrams of brittle structures: (left) normal faults (poles) and associated steeply plunging slickensides; (centre) strike-slip faults with dextral and sinistral kinematics; (right) extensional joints (poles). Projection to the lower hemisphere.*

6.3. Geochemistry

Nine rock samples were taken in the area of Shashemene sub-sheet and additional 1 sample in the nearby surroundings for geochemical analyses. For comparisons, analyses of 4 rocks from the neighbouring Hawasa sub-sheet (Rapprich et al. 2013) were also used. One sample (Sd042) represents Miocene Bale basalt, one sample Late Miocene–Pliocene Bofa basalt (Sd061 south of the sub-sheet), two samples represent Lower Pleistocene rhyolitic lavas of the Hawasa Caldera (Sd013 and Sd017), and four samples characterize Middle Pleistocene Corbetti Caldera (Sd036, Sd048, Sd067 and HSRVR010 from the Hawasa sub-sheet: Rapprich et al. 2013). The composition of the Middle Pleistocene Hawasa basalts (HSRVR035 and HSRVR177) has already been presented for the Hawasa sub-sheet (Rapprich et al. 2013), the samples were re-analysed in the CGS laboratories. One sample (HSRVR009) represents yellowish phreatomagmatic tuff and data from one sample of young Wendo Koshe pumice (Sd007) is compared with the analytical data of two samples (HSRVR041 and HSRVR069D) from the Hawasa sub-sheet. Due to failure of the ICP-MS machine in the CGS labs, trace element data for the samples HSRVR009, HSRVR035, HSRVR177, Sd042, Sd061 and Sd067 could not be completed before the compilation of this explanatory text.

In the TAS diagram (figure 6-25a) the analyzed basaltic rocks of the Nazret Group are plotted in the field of basalt or basaltic trachyandesite respectively. These rocks are weakly alkaline with sodium dominating over potassium (3.47–4.22 wt. % Na_2O vs. 1–1.27 wt. % K_2O). The basic, nearly intermediate composition is reflected in the moderate MgO content (5.5 and 1.35 wt. % respectively). The younger Bofa basalt (Sd061) seems to be of more primitive origin with an Mg# value of about 48 compared to 17 in the Bale basalt sample.

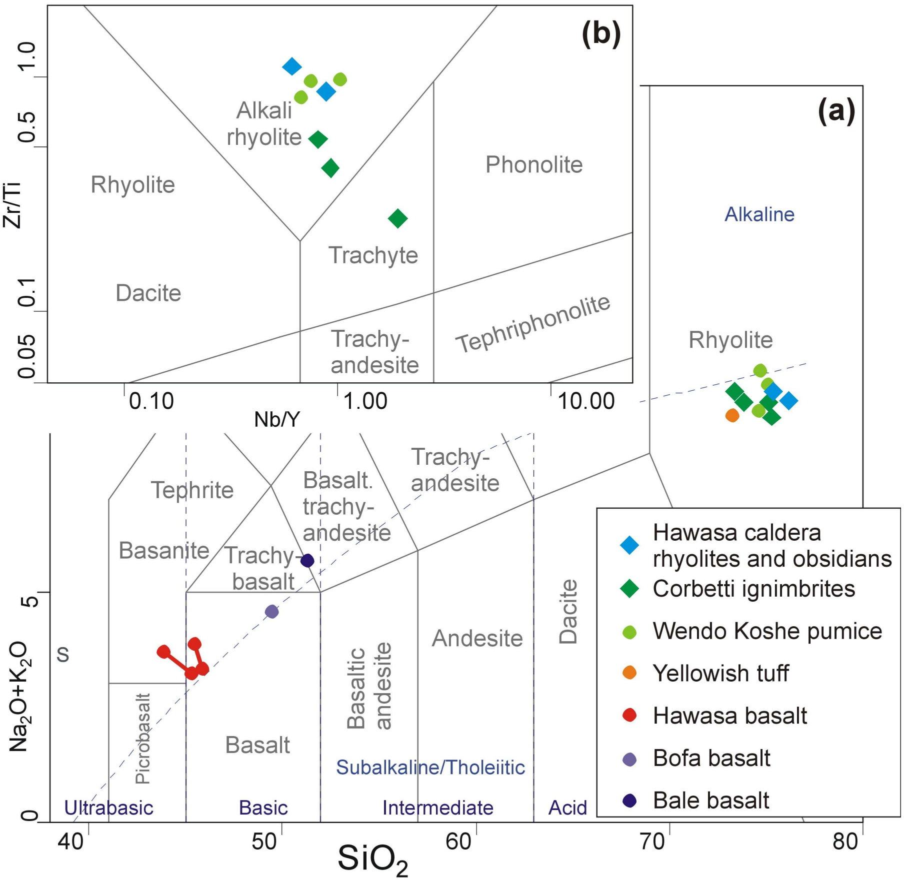

Figure 6-25. *Classification diagrams of analysed rocks: a) TAS diagram (Le Bas et al. 1986); b) Nb/Y vs. Zr/Ti diagram (Pearce 1996).*

Rhyolite lavas of the Hawasa Caldera are plotted in the field of rhyolite (figure 6-25a) or alkali rhyolite (figure 6-25b), respectively. These silicic (SiO_2 74.45–75.16 wt. %) alkaline (Na_2O+K_2O 9–9.23 wt. %) rocks are low in MgO (0.02–0.03 wt. %) and compatible elements (Cr ca 5 ppm, Ni 11–12 ppm).

The crystal-rich rhyolite (Sd013) appears more differentiated compared to the obsidian (Sd017) of the same formation in terms of trace element content. It is higher in less-compatible and lithophile elements such as Rb (143 ppm compared to 65 ppm in Sd017), Th (21 ppm compared to 12 ppm) and Zr (1452 ppm compared to 878 ppm). Sample Sd013 also has a pronounced Eu-anomaly (Eu/Eu* = 0.11 – figure 6-26).

Three samples of Corbetti ignimbrites (Sd036, Sd048, Sd067) are compared with sample HSRVR010 from the Hawasa sub-sheet (Rapprich et al. 2013). Even though all four samples are plotted in one narrow cluster in the rhyolite field in the TAS diagram (figure 6-25), the HSRVR010 sample differs in higher Nb/Y and lower Zr/Ti ratios suggesting a more trachytic tendency. In addition to lower Y and Zr concentrations (see Annex 1), this rock also differs also in lower REE content (ΣREE = 367.5 ppm vs. 605.4–719.8 ppm – figure 6-26) accompanied by significantly higher La_N/Yb_N ratio (11.15 vs 6.4–7.7 in other rocks of this unit).

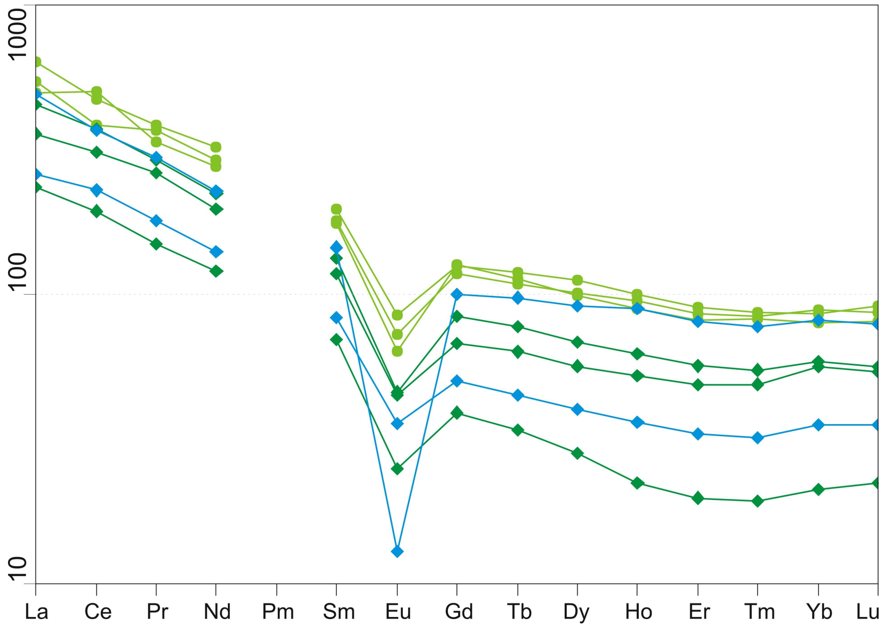

Figure 6-26. *Spider-plot of analyzed samples normalized to chondrite composition (Boynton 1984). Symbols correspond to figure 6-25.*

The new analyses of Hawasa basalts (HSRVR035 and HSRVR177) suggest lower silica content (only 43.46 or 44.82 wt. % respectively) and higher alkalis (3.6–3.8 wt. %) than obtained from the GSE analytical data. Analytical data for single samples are connected by a solid line in the figure 6-25a. Despite low silica content, low mg# values (37–52 for new analyses), low MgO content (5–8.44 wt. %) as well as low content of compatible trace elements (Cr = 30–36 ppm, Ni = 22–29 ppm) suggest that these basalts do not represent primitive melts.

The yellowish phreatomagmatic tuff (HSRVR009) also has a rhyolitic composition like the other silicic volcanic rocks in this area (figure 6-25a). All three samples from the Wendo Koshe pumice fall deposit are plotted within a narrow span in all of the diagrams suggesting an alkali rhyolite composition (figure 6-25). This pumice is characterized by an increased content of fluorine (0.2–0.25 wt. %) and a significant Eu- anomaly (ca 0.5 – figure 6-26).

6.4. Geochronology

Seven rock samples were analysed for K-Ar geochronological data in the ATOMKI laboratories of the Hungarian Academy of Sciences in Debrecen (table 6-1). The oldest of the analysed rocks (Sd042) yielded an age of 10.3 ± 1.4 Ma, suggesting the analysed basalt belongs to the lower part of the Nazret Group. Basaltic rocks of such a position are known as Bale basalts in the wider area. Similar ages (9.61 and 8.39 Ma) were obtained for basaltic lava embedded between rhyolitic ignimbrites of the Nazret

Group on the western scarp of the Main Ethiopian Rift, near Butajira and Kela (JICA 2012). Another basaltic rock sampled just south of the mapped sub-sheet (Sd061) yielded an age of 5.51 ± 3.8 Ma. This age corresponds to the basaltic unit in the topmost part of the Nazret Group known as Bofa basalts (e.g., Astatke and Šíma 2012). Ages of the rhyolitic lavas (Sd013 and Sd017) are of 1.18 ± 0.12 and 1.02 ± 0.14 Ma, respectively, suggesting effusive activity of the Hawasa Caldera post-dating the climactic ignimbrite forming eruption ca 1.28 Ma (JICA 2012). Several ages obtained from the Corbetti ignimbrites (Sd038, Sd048 and Sd067) document the multi-episode evolution of the Corbetti Caldera. The obtained ages suggest at least three ignimbrite forming eruptions 0.98 (± 0.26), 0.669 (± 0.129) and 0.2 (± 0.14) Ma. Even though the error of the last event nearly reaches the value of the age, this value is confirmed by the previously published ages of 0.19 and 0.21 Ma (JICA 2012).

Table 6-1. *K-Ar analytical results of dated samples from the Shashemene sub-sheet.*

Sample	K (wt. %)	$^{40}Ar_{rad}$ (ccSTP/g)	$^{40}Ar_{rad}$ (%)	K/Ar age (Ma)
Sd013	3.677	1.5522×10^{-7} 1.8434×10^{-7} 1.6978×10^{-7}*	12.7	1.18 ± 0.12
Sd017	3.448	1.3675×10^{-7}	10.4	1.02 ± 0.14
Sd036	3.715	9.6643×10^{-8}	7.2	0.669 ± 0.129
Sd048	3.849	2.9929×10^{-8}	2.1	0.20 ± 0.14
Sd042	0.822	3.3012×10^{-7}	10.3	10.30 ± 1.40
Sd061	0.813	1.7449×10^{-7}	2.1	5.51 ± 3.8
Sd067	3.568	1.3692×10^{-7}	5.2	0.98 ± 0.26

** replicated measurement of 40Ar, the average (third line) value was taken for further calculations.*

6.5. Geological evolution

Nazret Group volcanic rocks erupted during the Late Miocene and Pliocene. Rhyolitic ignimbrites were intercalated by at least two units of basalt to basaltic trachyandesite lavas (ca 10 and 5 Ma). Subsequently the Hawasa Caldera with a diameter of about 30 km formed in the mapped area. After the 1.3 Ma ignimbrite-forming eruption, several lava domes erupted along the caldera margins ca 1.2–1 M.y. ago. The original shape and scarps of the Hawasa Caldera were strongly modified by on-going tectonic activity on the marginal rift-faults. After the formation of the Hawasa Caldera, the new Corbetti Volcano began to emerge in its north-western sector (west of the mapped area) producing several ignimbrite units (<1, 0.67 and 0.2 Ma) during the Middle Pleistocene. The Hawasa Caldera was transected by a belt of basaltic lavas erupted through several scoria and tuff cones after the Corbetti ignimbrite-eruptions. These basaltic cones are often covered by younger silicic pyroclastic deposits. The yellowish tuff possibly erupted from the Fike Volcano, northwest of the mapped area. The latest volcanic rock is represented by Wendo Koshe pumice fall covering a large area in the western part of the sub-sheet. Already synchronously with post-caldera volcanism, the Hawasa Caldera started to be filled with polygenetic deposits comprising re-sedimented pyroclastics, as well as alluvial and lacustrine sediments. The prominent slopes are prone to slope deformations and therefore are rimmed with colluvial deposits. Ongoing hot-spring activity results in a continuous accumulation of travertines.

6.6. Geological localities

1. Hawasa scoria cone is exposes by a temporary quarry (figure 6-27, RP HSRVR125). This locality belongs to the Hawasa basaltic belt transecting the Hawasa Caldera. Accumulations of ill-sorted scoriae with a clast-supported structure as well as abundant spindle-shaped volcanic bombs can be well observed in the quarry.

2. Shashemene "cave" – cellars excavated during the last 30 years by a local inhabitant (figure 6-28, RP HSRVR175) provide exposure in the yellowish phreatomagmatic tuff in its entire thickness of about 6 m. In the walls and roof of the cellars, the various textures of the pyroclastic deposits suggest variable depositional processes comprising ash-flow, ash-cloud surge and ash-fall with accretionary lapilli. The base consists of 2 m thick massive matrix-supported ash-flow deposits followed by a sequence of alternating layers of fall and surge and another massive ash-flow deposit. The entire sequence is topped by well-developed brown-coloured fossil soil buried by about 1.6 m of Wendo Koshe pumice fall.

Figure 6-27. *Temporary quarry in the scoria cone. Photo V. Žáček.*

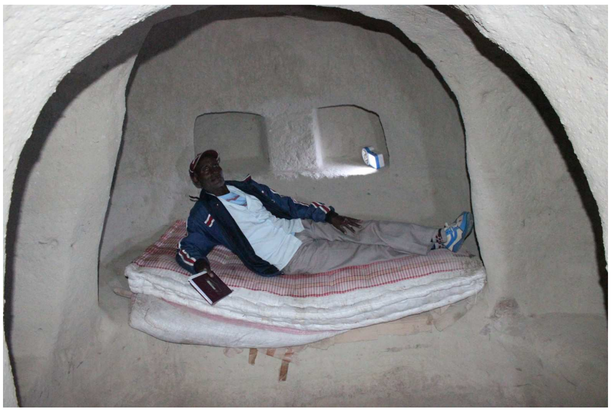

Figure 6-28. *Owner and creator of the cellars dug in the yellowish phreatomagmatic tuff. Photo V. Žáček.*

3. Sandpit near Shashemene Alaba-Kulito road (RP HSRVR009) is easily accessible from the asphalt road. This sandpit exposes more than 6 m of ash-fall deposits of yellowish phreatomagmatic tuff with abundant spectacular accretionary lapilli (figure 6-29). The tuff is also covered by ca 1.2 m of Wendo Koshe pumice fall.

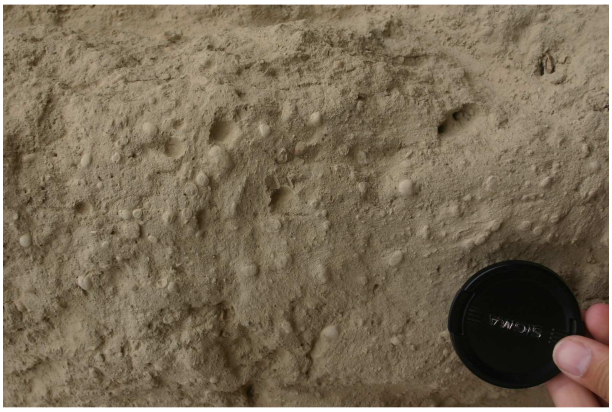

Figure 6-29. *Abundant accretionary lapilli in the yellowish phreatomagmatic tuff (RP HSRVR009). Photo V. Rapprich.*

Figure 6-30. *Shalo hot spring beneath the Weransa Ridge escarpment. Photo V. Žáček.*

4. Shalo hot spring is located below the Weransa Ridge. The hot spring is associated with the intersection of NW-SE and NNE-SSW trending faults. Two big and numerous smaller springs have a productivity of tens of litres of hot water per second (see more in the chapter Hydrogeology). The spring is not associated with travertines but other minerals precipitate from the hot water. The precipitate was identified using X-ray diffraction as a mixture of troona (hydrous sodium hydrogen bicarbonate) and kogarkoite (Na_3FSO_4).

5. Sole quarry (RP KV44) is a large active quarry (figure 6-31) located in the vicinity of Sole village to the east of Shashemene. The quarry exploits welded facies of Corbetti rhyolitic ignimbrite overlain by ca 2 m thick lateritized phreatomagmatic tuff. The ignimbrite contains well-visible fiamme, lithics and fragments of quartz crystals. The rock is very fresh and hard.

Figure 6-31. *Columnary jointed welded Corbetti ignimbrite overlain by lateritized tuff at Sole quarry. Photo V. Žáček.*

Figure 6-32. *One of the Wendo Genet hot springs with travertine cementing the colluvial deposits. Photo V. Žáček.*

6. Wendo Genet springs – a row of numerous hot springs can be found in the upper part of the Werke Brook Valley in the hills above Wendo Genet. The springs are located in colluvial deposits, where travertine precipitation causes cementation of loose deposits (figure 6-32) and creation of small travertine moulds.

7. HYDROGEOLOGY

The eastern part of the Shashemene area (about 50% of the sub-sheet) is located on the rift floor and has a subtropical (Weina Dega) climate. The western part of the area (about 50% of the sub-sheet) is located on the western escarpment and has a temperate (Dega) climate. Sedimentary formations and unconsolidated volcanic materials form the flat plain of the Hawasa Caldera and coherent (solid) volcanic rocks outcrop mainly in the escarpment area. Rocks are eroded by rivers forming deep gorges and valleys in the escarpment area. The rain gauges and annual rainfall averages are shown in Table 7-1. An average of 1,300 mm of rainfall was adopted for the Shashemene area.

Table 7-1. *Climatic stations of the Shashemene area*

Station	Class	Coordinates		Altitude [m a.s.l.]	Average rainfall [mm]	Sub-basin
		X	Y			
Hawasa	1	442915	780888	1,765	969	Hawasa
Shashemene	4	455884	795851	1,934	835	Shalla
Wendo Genet	4	457547	782775	1,765	1,135	Hawasa
Kofele	1	476356	782064	2,679	1,184	Wabe Shebelle

The Shashemene area is part of the Rift Valley Lakes closed basin and its sub-basins of the Hawasa and Shalla lakes. The south-eastern corner of the map belongs to the Wabe Shebelle basin. The Wesha, Werka Gomesho, and Wedesa rivers drain water from the eastern escarpment (eastern scarp of the Hawasa Caldera) and feed the swampy area of the former Lake Cheleleka (Shalo). Lake Cheleleka is drained by the Tikur Woha River which feeds Lake Hawasa (figure 7-1). The Debaba, Guta, and Denbi Rivers feed Lakes Shalla and Chitu.

The lakes represent the drainage basin of the area. They represent flooded calderas distinctly separated from the surrounding highlands and even the rift floor by steep mountain slopes. The maximum depth of Lake Hawasa is 20 m. Fluctuation in levels of Lake Hawasa has been measured since October 1969. The specific runoff of 12 l/s/km2 and 5 l/s.km2 for the escarpment and rift floor areas and specific baseflow of 6 l/s/km2 and 1 l/s.km2 for the escarpment and rift floor areas was adopted for the Rift Valley Lakes basin. The adopted average specific runoff and specific baseflow was 8.5 5 l/s.km2 and 3.5 5 l/s.km2 for the Shashemene sub-sheet. The main characteristics of the rivers of the Shashemene sub-sheet and rivers surrounding the Shashemene area are shown in table 7-2 and figure 7-1.

Table 7-2. *Main river characteristics*

River	Station	Mean flow [m^3/s]	Annual flow [mm]	Area [km^2]	Specific runoff [$l/s.km^2$]	Specific baseflow [$l/s.km^2$]*
Tikur Woha	Hawasa	6.6	?	?	?	?
Tikur Woha	Dato village	3.62	199	625	4.25	1.54
Butara /Werka	Near Wondo Genet	0.26	200	41	6.3	?
Wesha	Wondo Genet	0.63	197	40	15.8	13.3–15.3
Debaba	Kuyera	1.04	201	163	6.4	0.9-4.9
Guta	Melka Oda	0.32	135	75	4.3	?

**Specific baseflow was assessed by Kille and hydrograph separation methods.*

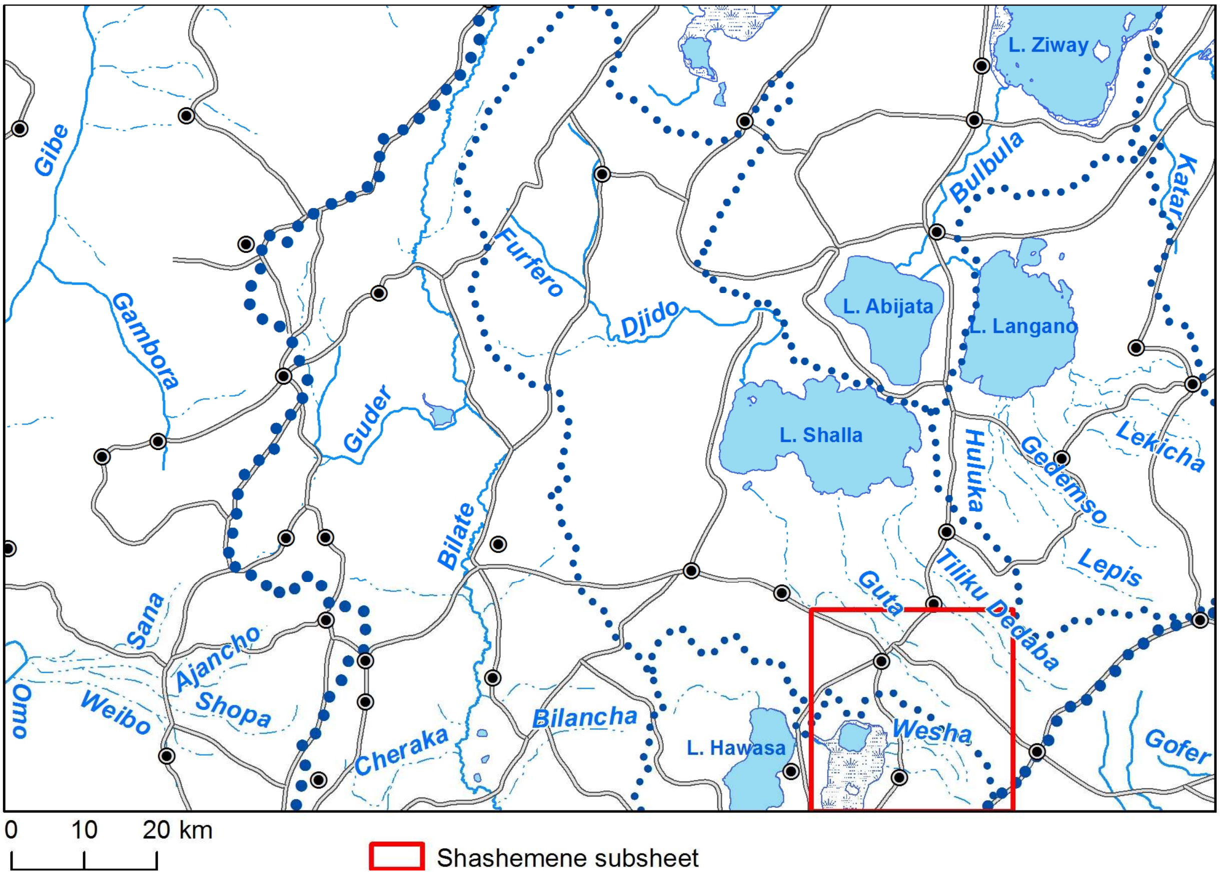

Figure 7-1. *The river scheme of the Hoseina 1:250 000 sheet (location of the Shashemene sub-sheet in red, surface water divides in dotted blue lines).*

7.1. Elements of the Hydrogeological System of the Area

The qualitative division of lithological units is based on the hydrogeological characteristics of various rock types using water point inventory data from the Shashemene map sub-sheet and from the surrounding area. The lithological units were divided into groups with dominant porous and fissured permeability and mixed permeability. This division served for a definition of the aquifer/aquiclude system of the Shashemene map sub-sheet. Since quantitative data such as permeability, aquifer thickness and yield are not adequate or evenly distributed enough to make a detailed quantitative potential classification, analogy was used for characterization of rocks without the adequate number of water points. The hydrogeological map shows aquifers and aquicludes defined based on the character of the groundwater flow (pores, fissures), the yield of springs and the hydraulic characteristics of boreholes. The following aquifers/aquicludes were defined:

1. Extensive and moderately productive or locally developed and highly productive porous aquifers (T = 1.1–10 m2/d, q = 0.011–0.1 l/s.m, with spring and well yield Q = 0.51–5 l/s). The aquifers consist of Quaternary polygenetic sediments (spQ) and alluvial, fluvial and colluvial sediments (aQh, fQh, cQh), and scoria (sbQp). The aquifers are shown in light blue.
2. Local and moderately productive fissured aquifers (T = 1.1–10 m2/d, q = 0.011–0.1 l/s.m, with Q = 0.51–5 l/s). The aquifers consist of basalts (bQp), basaltic lapilli-stone (lbQp), ignimbrite (igpQph), rhyolite (pQph, epQph) and trachyandesite (tbQph). The aquifers are shown in light green.
3. Extensive and moderately or locally developed and highly productive mixed porous and fissured aquifers (T = 1.1–10 m2/d, q = 0.011–0.1 l/s.m, with spring and well yield Q = 0.51–5 l/s). The aquifers consist of sequences of sedimentary, coherent volcanic rocks, pyroclastic rocks and ignimbrite pumice fall (igpQc, ppQwf, tpQpc, bpQpc), and the underlying Nazret Formation (igpN) which is only show on the hydrogeological scheme. The aquifers are shown in light green and light blue horizontal hatching.
4. Formation consisting of a minor fissured aquifer with local and limited groundwater resources – Aquiclude. The formation consists of Hawasa obsidian (opQph). The rocks are shown on the hydrogeological map in light brown.

7.1.1. EXTENSIVE AND MODERATELY PRODUCTIVE POROUS AQUIFERS

Extensive and moderately productive porous aquifers cover about 145 km^2 (20%) of the sub-sheet area. Porous aquifers are aquifers where groundwater is accumulated in and flows through pores of an unconsolidated or semi-consolidated material. Classical porous unconsolidated sediments of the Quaternary age are represented by polygenetic material, including re-sedimented pyroclastics and lacustrine sediments around lakes (Hawasa and Cheleleka) and alluvial, fluvial and colluvial sediments. Particularly lacustrine sediments around lakes can reach a thickness of several tens and even hundreds of meters. Scoria cones also represent material with dominant porous permeability, but they are relatively small with steep slopes and their hydrogeological activity is minimal. The rocks with porous permeability forming aquifers are expressed on the hydrogeological map in blue.

A porous aquifer on the western shore of Lake Cheleleka is large and thick and its groundwater is developed by a large number of drilled and dug wells in Hawasa town. The porous aquifer is a very good source of groundwater depending on the thickness, sorting and recharge conditions. Lacustrine sediments and re-sedimented pyroclastics are mainly recharged by direct infiltration by percolating rain water, but can be also recharged by bank infiltration during floods with high levels of water in river channels as well as in lakes. Deep regional groundwater flow from the eastern highlands and escarpments can also recharge lacustrine sediments and re-sedimented pyroclastics in the depression of lakes Hawasa and Cheleleka by lateral flow.

Volcano-sedimentary rocks are developed in shallow depressions and are generally represented by volcaniclastic strata associated with volcanic eruptions, which have hydrogeological characteristics of sedimentary materials. Small scoria cones in the western part of the sub-sheet also represent material with dominant porous permeability. These are dominated by clastic sediments of a volcanic origin intermixed with lacustrine and fluvial units and tuff materials. Moderate yields may be found locally where the aquifer provides important local supplies.

The yield of boreholes drilled to the aquifer varies from 1 to 5 l/s. The average thickness of the aquifer is about 50 m but we can say that the thickness varies from 40 m to more than 200 m. The frequency of yield of water points from porous aquifers of the Shashemene sub-sheet and its surroundings as well as their basic statistics are given in table 7-3.

Table 7-3. *Basic statistics of yield of water points from porous aquifers in l/s*

Number of data sets	Max	Min	Median	Average
90	75	0.029	2.5	4.61

Drilled wells in this aquifer on the Shashemene sub-sheet were observed to strike groundwater at a depth of 10–80 m with discharge of 2.7 to 8.3 l/s for the wells. There are also some shallow wells and dug wells taping the shallow groundwater, despite the fact that most of the shallow wells have a high content of fluoride and relatively high value of TDS when drilled nearby Lake Hawasa. The fluoride content is particularly high when thermal water is struck by the well.

7.1.2. LOCAL AND MODERATELY PRODUCTIVE FISSURED AQUIFERS

Fissured aquifers developed in coherent volcanic rocks cover 12 km^2 (1.5%) of the sub-sheet area. Fissured aquifers are aquifers where groundwater accumulates in and flows through the weathered and fractured parts of volcanic rocks. The porosity of lava flows may be high but the permeability is largely a function of a combination of the primary (pores) and secondary structures (joints and fissures) within the rock. In addition, the permeability of lava flows tends to decrease with geological time. The pyroclastic rocks between lava flows are generally porous but usually less permeable due to poor sorting. They can be represented by impermeable non-welded tuffs in some parts of the volcanic sequences. Hence, extensive volcanic ash beds may form semi-horizontal barriers to water movement (infiltration) resulting in lower productivity of basaltic units located at greater depth. Layers of paleosoils of various thicknesses in between lava flows are also less permeable and usually consist of clay material on the one hand, whereas layers of fluvial and lake sediments and pumiceous pyroclastic deposits between individual lava flows can enhance well yield on the other hand.

Quaternary volcanic rocks like basalt, basaltic lapili-stones, rhyloitic ignimbrite, rhyodacite, rhyolite and trachyandesite have dominant fissured permeability and represent fissured aquifers of the sub-sheet. The units with fissured permeability forming moderately productive aquifers are expressed on the hydrogeological map in light green.

Welded ignimbrites usually alternate with non-welded facies and are interbedded with tuffs, pumice and lacustrine or alluvial deposits. Groundwater flows through joints, fractures and pores of non-welded layers and interbedded sediments, however fissure flow is the dominant hydrogeological characteristic of these rocks. Open faults and fault systems may also provide significant groundwater flow paths, which may allow regional transfer of groundwater where they are extensive.

Outcrops of ignimbrites are mostly well jointed providing good possibility for direct infiltration as well as indirectly by overlaying porous aquifers within the Corbetti sequence. The continuity of fractures in both horizontal and vertical planes provides the aquifers their hydraulic continuity with adjacent units and aquifers. Yields from both boreholes and springs may vary widely. The basic statistics of the yield of water points of fissured aquifers of the Shashemene sub-sheet and its surroundings area are shown in table 7-4.

Table 7-4. Basic statistics of yield of water points from fissured aquifers in l/s

Number of data sets	Max	Min	Median	Average
190	70	0.035	3	4.67

Wells developing groundwater from fissured aquifers located on the Shashemene sub-sheet have a yield ranging from 0.3 to 18.3 l/s, documenting the moderate productivity of the aquifers. The groundwater level is about 20 to 60 m below the surface in the western part of the sub-sheet. The level of groundwater is between 15 and 30 m below the surface at the foot of escarpment in the eastern part of the sub-sheet, but can vary significantly based on the topographical position of the drilled wells in the escarpment area. The yield of springs in the eastern part is about 7 l/s.

7.1.3. EXTENSIVE AND MODERATELY PRODUCTIVE MIXED POROUS AND FISSURED AQUIFERS

Mixed aquifers developed in volcanic rocks cover 558 km^2 (77 %) of the sub-sheet area. Volcanic rocks in the Rift Valley are often mixed with sediments accumulated by rivers and lakes in between lava flows of different volcanic episodes. The rocks are also intercalated with relatively thick layers of non-welded tuffs, ash-flows and pumiceous pyroclastic deposits. These intercalated porous materials do not act as independent aquifers but they form a mixed fissured and porous multilayered aquifer together with the volcanic rocks. Porous materials can significantly contribute to the safe yield of wells when they are developed together with volcanic rocks. The permeable porous sediments in between lava flows form a body that can accumulate large volumes of groundwater by draining the surrounding fissured aquifers and contribute to the yields of wells developing groundwater from this mixed aquifer, which is more productive than fresh basalt, ignimbrite, trachyte and rhyolite that are normally considered as rocks with moderate and/or low permeability.

Wendo Koshe pumice fall with subordinate flow deposits and phreatomagmatic tuff covering large areas of the north-western part of the sub-sheet have porous permeability, but they are compacted in some parts which shows combined fissured and porous permeability. These two lithological units are several meters thick and generally do not represent individual aquifers. They are connected with underlying aquifers developed in ignimbrite, which are also frequently intercalated with various sedimentary and pyroclastic porous materials. All of these lithological units together represent large and thick multilayered aquifers with combined porous and fissured permeability. Neogene volcanic rock of the Nazret Group also forming a mixed aquifer underlies outcrops of volcanic rocks of the sub-sheet. The units with mixed permeability forming moderately productive aquifers are expressed on the hydrogeological map in light green and light blue horizontal hatching.

The mixed aquifers are exposed in the northern part of the sub-sheet where they form gently sloping eastern to north-eastern plains of the rift floor and in the eastern part of the sub-sheet where they form the eastern escarpment.

The aquifers are recharged directly by percolating rain water as well as indirectly by overlaying porous aquifers of the Corbetti complex. Aquifers show both watertable and confined aquifer systems. The basic statistics of the yield of the water points of the Hawasa sheet and its surroundings area are shown in table 7-5.

Table 7-5. Basic statistics of yield of water points from mixed aquifers in l/s

Number of data sets	Max	Min	Median	Average
132	78	0.01	2	4.84

Wells developing groundwater from mixed aquifers located on the map have a yield between 0.3 to 2.2 l/s, documenting the moderate productivity of the aquifer. The groundwater level is about 20 to 50 m below the surface in the western part of the sheet. The level of groundwater is between 100 and 150 m below the surface in the elevated eastern part of the sheet, but can vary significantly based on the topographical position of drilled wells in the escarpment area. The yield of springs in the eastern part is from 0.03 to 15 l/s.

7.1.4. FORMATION CONSISTING OF A MINOR FISSURED AQUIFER - AQUICLUDE

Volcanic rocks with local and limited groundwater resources - Aquicludes are units where groundwater is neither stored nor transmitted through the rock. Groundwater development for limited individual water supply is very difficult and even impossible in places. These are groundwater resources with poor or no exploitation potential and are represented by Hawasa obsidian. The fissures in the obsidian are well developed but they are open and the infiltrated water is transmitted very fast and the unit has no ability to store water. The units with limited groundwater resources are expressed on the hydrogeological map in light brown.

7.2. Hydrogeological Conceptual Model

The general concept of infiltration and groundwater circulation on the Shashemene sub-sheet consider the relevant parts of the rift floor, the eastern highlands and the escarpment area.

The eastern plateau area is covered with various volcanic rocks forming a gently undulating plain that receives adequate rainfall and has moderate runoff resulting in good infiltration and the formation of extensive and moderately productive or locally developed and highly productive fissured and mixed aquifers. Infiltration is particularly good in areas where the plateau is covered by thick eluvias and laterites. Aquifers outcropping in the plateau area also feed deeper fissured aquifers developed in underlying volcanic and sedimentary rocks. The escarpment area is relatively steep for infiltration; however, some of its parts provide a good opportunity for water to percolate underground and feed the aquifers on the escarpment as well as rift floor. The groundwater flow system and direction in the escarpment area are mainly controlled by its faults. There are also some faults which seem to act as barriers to flow and some faults are used by hot water to circulate from deep regional flow to the surface, where it emerges as hot springs in Wendo Genet and other areas. The escarpment is a part of the hydrogeological system of the Rift Valley providing a transfer of groundwater from the highlands to the rift floor.

Springs at the foothills of the escarpment are large and there are even hot springs at Wendo Genet and Shalo representing deep local and/or regional groundwater flow. Groundwater flowing from the eastern escarpment feeds the aquifers developed in volcanic and sedimentary rocks of the rift bottom. Local ridges on the rift floor generate shallow local groundwater flow and form local groundwater divides which conform to the surface water divides. This shallow local as well as deep groundwater flow recharges the lacustrine sediments of lakes which form regional drainage of the Rift Valley Lakes basin. Lake Hawasa represents drainage of the south-western part and Lake Shalla represents drainage of the north-western part of the sub-sheet. It is also possible that the lacustrine sediments are recharged from rivers and lakes when the water level in the rivers and lakes is higher than the surrounding groundwater level in the aquifers. A conceptual hydrogeological model is shown in figure 7-2.

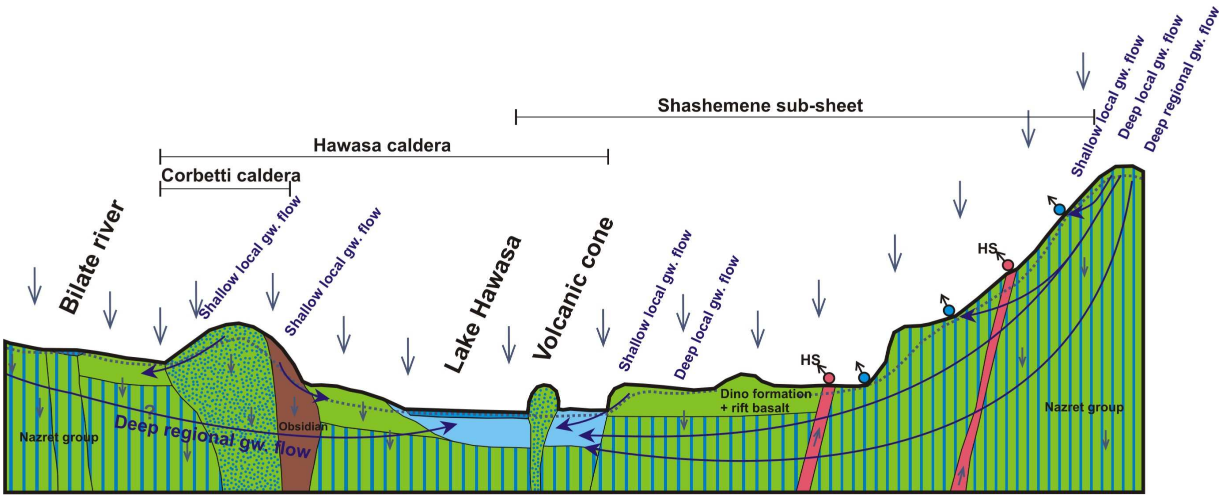

Figure 7-2. *Conceptual hydrogeological model of the Shashemene area.*

The principles of the general conceptual model of the Shashemene sub-sheet are based on the main mechanisms of recharge as well as discharge as follows:

- direct recharge to outcropping aquifers
- vertical recharge from overlying aquifers into underlying aquifers
- horizontal recharge from neighbouring aquifers, rivers and lakes
- direct discharge by springs from outcropping aquifers (cold and hot springs at the foot of the escarpment and the rift floor)
- direct discharge to rivers and lakes
- indirect discharge from one aquifer to another (vertical as well as horizontal)

Groundwater is under watertable conditions; however, artesian conditions are also known from the mixed volcano sedimentary aquifers of the plateau, escarpment and rift floor.

Groundwater flow is in general parallel with the surface water flow system and is from the highlands through the escarpment to the rift floor. On the rift floor itself, the groundwater flow direction is governed by the relative elevations between the individual sub-basins and elevation of the lakes Hawasa and Shalla.

Groundwater (drilled and dug wells) remains the main source of water supply for towns and villages within the Shashemene sub-sheet. Halcrow (2008) estimates groundwater makes up 92 % of the water supply.

7.2.1. ANNUAL RECHARGE IN THE AREA

There is a large volume of data from different reports about the assessment of recharge; however, these data vary significantly. The regional mechanism of recharge of aquifers in the area has been described above. As is the case in other areas the groundwater is recharged from precipitation depending on its intensity and annual distribution, topographical gradient of the area, as well as the lithological composition (particularly in vertical profile) of outcropping rocks and their permeability. A substantial part of the groundwater is recharged from direct precipitation. There is also a seasonal but less significant amount of recharge to localized aquifers from the permanent as well as intermittent streams and lakes after rains when the level of water in rivers and lakes is above the groundwater level in the surrounding aquifers.

Tesfaye (1993) characterized recharge to be less than 150 mm in the highland and between 70 to 100 mm in the rift basin based on baseflow data of Katar and Meki rivers. Recharge based on rainfall infiltration according to the rainfall infiltration factor (RIF) was defined by WWDST (2003) to be about 6 % for alluvium and basaltic rocks if the slope of the terrain is less than 20 %.

Tadesse and Zenaw (2003) assessed recharge for the Hawasa basin to be about 5 % of the rainfall (67 Mm^3/year). WABCO (1990) in Water Resources Development Master Plan for Ethiopia refers to 5 % recharge to the aquifers in RVLB representing about 57 mm of annual recharge.

Taking into consideration the variation of baseflow values for the rivers in highlands, escarpment and the rift floor, the recharge is about 200 mm and 50 mm. Compared to the adopted average depth of precipitation of 1,300 mm the calculated average infiltration (recharge) can be assessed as being 104 mm or 8 % of the precipitation depth.

7.2.2. HYDROCHEMISTRY

A study of the groundwater quality was carried out on the different aquifers (geological formations) of the area. The results of the hydrochemical study can help to understand the groundwater circulation within the aquifers in addition to comparing the water quality with various standards. A total of 34 water samples from cold and hot springs, boreholes and dug wells were analyzed for chemical composition. One sample was taken from surface water of the Tikur Woha River. The analytical results were presented graphically on a hydrochemical map (inset map) to facilitate visualization of the water chemistry, TDS and fluoride content. Suitability of groundwater for drinking, industrial and agricultural purposes is assessed based on the pertinent quality standards.

CLASSIFICATION OF NATURAL WATERS

Hydrochemical types are classified based on the Meq% representation of the main cations and anions. Basic hydrochemical type is the only type in the area and its content of the main cation and anion is higher than 50 Meq%. This chemical type is expressed on the hydrochemical diagram by a solid colour.

The hydrochemical types of groundwater in the study area are calcium-bicarbonate and sodium-bicarbonate. The type of groundwater within the Rift Valley Lake basin depends on the morphological position of the aquifer and whether it is located on the plateau ($Ca\text{-}HCO_3$ basic and transient), escarpment ($Na\text{-}HCO_3$ transient and basic) and/or rift floor ($Na\text{-}HCO_3$ basic). Groundwater residence time along flow paths, length of water-rock interaction, lithology, ion exchange, and evaporation may play a significant role in the increment of TDS in groundwater composition. The contact of water and hot rocks, including groundwater enrichment by carbon dioxide, is believed to form the sodium bicarbonate groundwater chemistry of the majority of the groundwater on the rift valley bottom. An important interaction is the leaching of fluoride from acid volcanic rocks, mainly from obsidian and rhyolitic pumice. The chemistry of groundwater in the Shashemene area reflects it position on the highlands, escarpment and rift floor and changes from transient $Ca\text{-}HCO_3$ type at higher altitudes of the escarpment into transient at lower altitudes of the escarpment and basic $Na\text{-}HCO_3$ type on the rift floor. To facilitate the visualization of the classification of water types, the percentage of the major cations and anions of the analysed samples is plotted on the Piper diagram shown in figure 7-3.

The same development as in groundwater types is observed in total of dissolved solids where groundwater with low TDS (less than 200 mg/l) is found in the highlands and the upper part of the escarpment in the eastern part of the map. It indicates the fast hydrogeological regime of the area receiving a relatively high volume of precipitation and where groundwater flows in young fractured volcanic rocks. Higher TDS of cold groundwater (between 200 and 1,000 mg/l) as well as higher content of fluoride (between 2 and 6 mg/l) in the western part of the sub-sheet indicate a slow hydrogeological regime in the drainage area where the groundwater flows mainly in various aquifers of the rift floor. TDS of hot water can reach nearly 3 g/l with fluoride content between 1 and 40 mg/l.

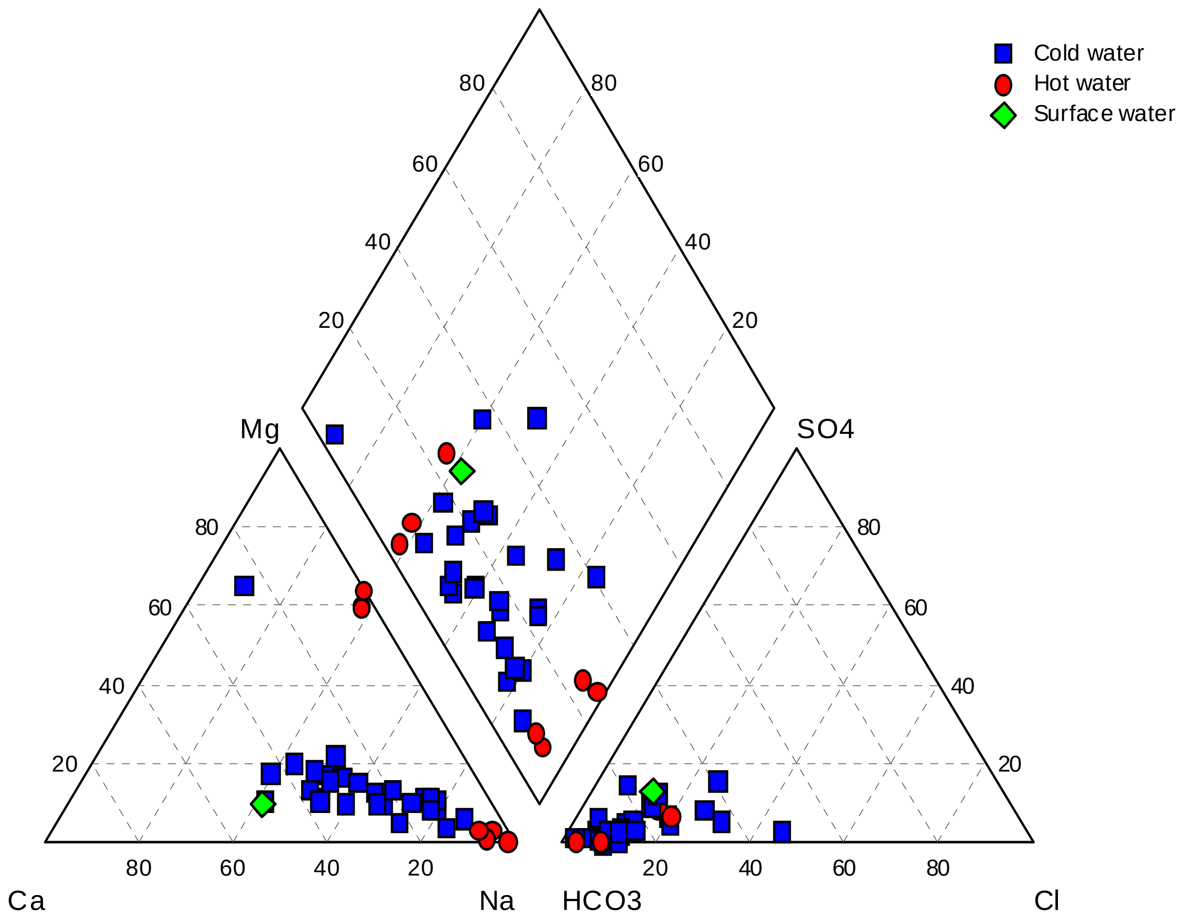

Figure 7-3. *Piper diagram for classification of natural waters.*

The water of the Tikur Woha River is also of basic Na-HCO3 type but has lower TDS (397 mg/l) than the groundwater in the lacustrine sediments.

WATER QUALITY

Water quality of the mapped area was assessed from the point of view of drinking, agriculture and industrial use.

To assess the suitability of water for drinking purposes, the results of the chemical analyses were compared with the Ethiopian standards for drinking water published in the Negarit Gazeta No. 12/1990 and the Guidelines of Ministry of Water Resources (MoWR, 2002).

Results of chemical analyses show that groundwater of the Shashemene area is good for drinking in the eastern part of the sub-sheet but is not convenient for drinking because of high fluoride content in the western part of the sub-sheet. Fluoride content usually exceeds the maximum permissible level (1.5 mg/l) in porous aquifers hosted by lacustrine sediments and mixed aquifers in the western part of the sub-sheet and in hot groundwater.

Agricultural standards for the quality of groundwater used for irrigation purposes are determined based on the Sodium Adsorption Ratio (SAR), total dissolved solids and United States Salinity Criteria (USSC). The Sodium Adsorption Ratio (SAR) is good to fair for irrigation with moderate salinity. There is no limit for the use of groundwater for livestock watering.

Groundwater is not suitable for direct use in most industries without the appropriate pre-treatment.

7.3. Thermal Water

Thermal water is very common in the Rift Valley. Hot springs are known in the Shashemene sub-sheet in the Wendo Genet and Shalo (Chelelaka) areas. Hot water is known from wells drilled along the main road from Dila to Hawasa. There is also the prominent hot spring of Graha Quhe located a few kilometres to the south of the border of the sub-sheet. A detailed geochemical study of thermal waters in the area is presented in a study of UNDP (1971) and the following text is taken from this study.

Hawasa geothermal area is represented by two groups of springs emerging along faults at the bottom of the Main Ethiopian Rift. Two spring groups i.e. Shalo and Graha-Quhe are hot springs located in the bottom of the Hawasa caldera at the margin of the swamp which is a remnant of the former Cheleleka Lake.

Shalo springs (figures 7-4 and 7-5) are located at the foot of Weransa Ridge and two groups of springs form the eastern and western arms of the small lake where gas rises in considerable quantity. This small lake is a part of the larger but not permanent Lake Cheleleka. Spring UHS-48 was said to be the hottest in the area and was hot enough to boil an egg. Around August 1970 the spring was excavated and dammed (the head was raised approx. 0.3 meter) to form a bathing pool. This caused the temperature to drop to 43 °C, and the discharge to cease. The water of the spring has recently been developed and water is pumped to the west and used for water supply of Gotu Onoma (Wesha) town (spring condition during the visit on the 12th of June, 2012). Spring UHS-52 is 150 m west-southwest of the spring UHS-48; it is one of the second group of springs and is close to the area where gas rises in the lake and only a few cm above the level of the lake. It emerges through sand, and is about 20 cm in diameter. The hot water lake is shown in figure 7-4. Clear water splashes up 5 cm high (temperature 96 °C), but there are no sinter deposits and the discharge is only 0.1 l/s. Di Paola (1976) states that the discharge from this group of springs is “not calculable, but high”. No springs with significant surface discharge were observed during this survey but hot water enters Lake Cheleleka (Shalo) at the position of the gas emission. The potential for hot water is high in this area.

Figure 7-4. *Shalo hot water lake. Photo J. Šíma.*

Figure 7-5. *Shalo hot spring. Photo V. Žáček.*

Hot springs of Graha Ricata in Graha-Quhe Wereda emerge close to the watertable on the northern and eastern base of a small rhyolite dome on the south-eastern edge of a swamp (Lake Cheleleka). The area is accessible from the main road to Wendo Genet. Very few springs can be approached closely because of their hot swampy surroundings. On the northern side of the dome spring UHS-2, 0.6 m in diameter and 10 cm deep, discharges 0.7 l/s of clear natural water at a temperature of 70 °C. There are no mineral deposits but there are algae growths in the overflow channel. Spring UHS-3 emerges at the east-south-east base of the dome. It is 0.2 m in diameter, and “boils” up to 5 cm high from amongst rhyolite blocks which have been placed over the vent. The temperature is 89 °C and the flow is 0.1 l/s. A few meters west, Spring UHS-4 also ejects water 5 cm high. Its eye, also infilled with blocks, is around 0.8 m in diameter. The surface temperature is 87 °C and discharge is

1.0 l/s. At both springs UHS-3 and UHS-4 some nodular buff and white coloured sinter encrustation blocks are wetted by splashing. The eastern group of springs (Spring UHS-2 and UHS-3) is used for inhalation and for drinking of hot water to treat bronchitis. The measured discharge of 2.0 l/s from accessible springs at Graha-Quhe represents only a fraction of the total discharge, most of which emerges directly in the swamp. The total discharge is estimated to be at least 10–15 l/s.

The Wendo Genet group represents springs located along the eastern escarpment several hundred meters above the plain. Belle hot springs just west of the Shashemene road near the north-eastern boundary of Wendo Genet farm are the source of Belle Stream. Springs UHS-38–43 and UHS-40 are collectively known as Belle Springs. They deposit travertine; in the past spectacular 2 m high cones were built but now the water emerges from holes in the base of the disintegrating cones. Spring UHS-38 and UHS-39 are the hottest (71 °C) and deposit limonite close by their vents, but the other four springs and innumerable small seepages deposit only travertine sinter which forms an apron, partly overgrown by sedges, extending southwards to the bank of Belle Stream. Here, discharge of 2.0 l/s supplies two bath houses.

Many hot springs at Kike (known as Wendo Genet Springs), located to the east of Wendo Genet, discharge water on the right bank of the Washa River, with some up to 40 meters above the river-bed. Two of the higher springs supply large swimming pools (Spring UHS-44, source of the eastern-most pool). The waters are clear, and extensively deposit travertine and limonites near their sources. Temperatures range from 67 to 69 °C and the total discharge is approximately 6.5 l/s. Both the Wendo Genet and Kike springs emerge on an east-west fault within the Wendo Genet Caldera, the former on the floor, and the latter high on the caldera wall. Other hot springs emerging further south at a similar elevation to Kike are known as Kenteri (Spring UHS-45), but permission was refused to observe them. There are said to be six hot springs with similar temperatures and total discharge similar to the Kike springs. The last spring in this area is known as Dobicho (Spring UHS-46). The Dobicho hot springs, situated south of Kenteri, issue from below a thick ignimbrite sheet in a gully cut back into the scarp end, draining the highlands beyond. There are more than 20 sources and the larger ones are used for bathing by the local people. These springs discharge a total of 10 l/s at a temperature of 43 °C.

Representative samples of the Hawasa and Wendo Genet areas were collected to the east of Lake Hawasa. Three samples (UHS-4, UHS-40 and UHS-52) were taken from springs discharging to a swampy plain, and two samples (UHS-44 and UHS-46) from springs in the escarpment to the east. In general these five samples show low Cl/total carbonate species (< 0.14), low Cl (< 130), and low FBO_2 content. Except for Spring UHS-12, these waters are also characterized by low fluoride content (although Cl/F ratios are low), moderate Ca and Mg content and generally low Cl/SO_4 ratios. The springs also have certain differences. Those on the plain have higher temperatures (96, 87, 68 °C) than those of the escarpment (43, 69 °C) and a lower rate of flow. SO_4 content is much higher in the former, and this is also true to a lesser degree for Cl, Br, I, Li, HBO_2 and H_2S. Even for major constituents HCO_3 and Na, the springs on the plain are mineralized, and have TDS nearly 3 times higher than that of the springs on the escarpment. Furthermore, Spring UHS-40 (Belle Spring) has the lowest Na/Li ratio in the lakes district and the highest Cl/F ratio in the group.

These chemical analyses can be interpreted in several ways. Firstly, it is likely, because of the solids, that Springs UHS-44 and UHS-46 are meteoric with a short underground residence time, and that water of Lake Shalla is derived from the same source. The abundance of HCO_3 and low fluoride seems to confirm the shallow nature and low temperatures of these waters. Secondly, springs UHS-4, UHS-40 and UHS-52 may receive steam from a deeper source, warming shallow HCO_3 waters. However, this hypothesis does not adequately explain the relatively high Cl and K content of these springs. Perhaps as an alternative to steam heating, hot (Na–K)–Cl waters escaping from a deep reservoir ascend to mingle with bicarbonate waters. This would better explain the high subsurface temperatures inferred from Na/K ratios, but it fails to explain the 118 °C differences in subsurface temperatures derived by the SiO_2 method and by N/K ratios for Springs UHS-44 and UHS-46.

The waters in the more highly mineralized springs UHS-4, UHS-40 and UHS-52 probably give a better indication of the subsurface conditions although they probably contain some shallow groundwater as indicated by the high magnesium contents. Temperatures of 150–200 °C may be found especially near

Spring 40. However, steam heating and some mixing with surface water renders these estimates only an approximation.

The low mineralized springs UHS-44 and UHS-46 are highly diluted which suggests that the Na/K ratios are strongly out of equilibrium in these lower temperature sodium and calcium bicarbonate waters. This is supported by their similarity to Lake Hawasa water. The cold shallow wells are similar to the hot springs (UHS-4, UHS-40 and UHS-52) of the plains in their degree of mineralization. Their colder temperatures result in lower Na/Ca, Cl/F and higher Na/Li ratios. Lake Hawasa appears to be fed principally by water similar to that discharged by strongly flowing springs on the escarpment to the east, with a minor subsurface contribution from the aquifer which supplies springs in the plain, and is tapped by the shallow wells. The chemistry corroborates the hypothesis that it is fed predominantly by direct runoff from rainfall on the highlands to the east of the eastern Rift escarpment, and from springs on the eastern escarpment that discharge a similar type of water of short underground residence time. The lake has no surface outlet. In the east, groundwater flow towards the lake is indicated by similarity in chemistry between spring waters at Graha-Quhe and wells near the eastern lake shore. Hence, subterranean discharge from the lake is probably confined to the south through west to north quadrants. It is conceivable that this could be the source of the Wagere springs and springs on the south-western shore of Lake Shalla.

Two occurrences of travertine associated with hot-springs in the Wendo Genet area were sampled for Sr-isotopic ratios (table 7-6). As the geochemical behaviour of Ca is close to Sr (e.g., Faure and Mensing, 2005), the detected source of Sr should also identify the source of Ca. The Sr isotopic signature for the travertine samples (ca 0.7045) is close to the composition of basaltic rocks within the Main Ethiopian Rift (ca 0.703–0.7045: Stewart and Rogers 1996, George and Rogers 2002). The Sr is not likely to be derived from the sedimentary rocks of the eastern plateau (Urandab, Gabredare and/or Hamanlei limestone) because the Sr isotopic composition of marine sediments of the age ranging from the Upper Jurassic to the Paleocene is in the span of 0.7068–0.7079 (McArthur et al. 2001, Veizer et al. 1999), well above the values measured. Similarly, much higher Sr-isotopic ratios should be expected for the crystalline rocks of the East-African upper crust due to the high time-integrated content of the radiogenic strontium. The rhyolitic ignimbrites surrounding the hot-springs with travertine are very poor in Ca and Sr and therefore could not represent the source of the carbonate precipitated in travertine heaps. The Sr-isotopic ratios much better fit to the mafic volcanic rocks and hence the origin of the fluids responsible for the precipitation of travertine may be related to the primary magmas or dissolution of the pre-rift or rift basalts underlying the Late Miocene to Pliocene rhyolitic sequences. However, this ratio confirms deep circulation of groundwater in the escarpment area.

Table 7-6. *Sr-isotopic ratios in travertine of Wondo Genet hot springs*

Sample	North	East	$^{87}Sr/^{86}Sr$	2 std. err. of the mean
HSRVR178	07.110354	38.614162	0.704500	0.000011
Sd023	07.078633	38.645062	0.704814	0.000013

7.4. Environmental Isotopes

The environmental isotopes analyzed in the study area for hydrogeological purposes are oxygen-18, deuterium, carbon-13 and radioisotopes: tritium and carbon-14. These isotopes together with chemical analysis data contribute to the understanding of:

- Recharge processes, rate and source
- Residence time of groundwater in the hydrogeological system
- Construct conceptual models and calibrate numerical models

The Local Meteoric Water Line (LMWL), $\delta^2H = 7.5 \times \delta^{18}O + 13.3$, established by this study (Tadesse and Zenaw 2003) has been applied to interpret the stable isotope data. Almost all of the samples from shallow wells including samples taken from Lake Hawasa are plotted along a line which is significantly shifted to the right of LMWL. This line, $\delta^2H = 5.5 \times \delta^{18}O + 7.6$, represents the evaporation line for the study area.

By applying the equation obtained from the relationship of oxygen-18 versus elevation, the major recharge elevation of about 2,000 m a.s.l. was calculated. A similar elevation (2,100 m a.s.l.) was also assessed based on the relation of elevation with rainfall and evaporation as an elevation from which rainfall prevails over evapotranspiration. This assessment confirmed the hypothesis about massive infiltration in the highlands and lower infiltration of rain water in the rift floor.

JICA (2012) also states that the majority of groundwater in the study area originates from rainfall because values are in the proximity of a meteoric line. Probably, the low value of δ presents the elevation effect of the origin, whereby most of the rainwater is infiltrated in the eastern highlands.

Tritium values of all of the samples range between -0.52 and 4.8 TU. Very low TU is related to deeper groundwater (boreholes and springs), whereas shallow water points including the water of Lake Hawasa show relatively higher tritium values. Generally, tritium activity decreases along the flow path whereas TDS values increase. However, in the study area the direction of flow inferred from TDS values is not supported by the tritium values because high tritium is related to high TDS and vice versa. This may suggest that the higher mineralization is not due to longer residence time along the flow path, but a high evaporation rate. The effect of evaporation on shallow dug wells is clearly depicted by the relationship between deuterium and oxygen-18. The high TU value (3.8) for Lake Hawasa may suggest that the lake is predominantly feed by surface runoff.

7.5. *Water Resources*

Water resources of the area depend mainly on rainfall and other climatic characteristics, as well as the hydrological, geological and topographical settings of the study area. As part of an integrated water resource and development program the use of surface and groundwater must be dealt with keen interest in addressing the acute problems of adequate and safe water supply schemes in the study area.

The long-term mean annual rainfall of the area has been assessed to be about 1,300 mm/year. For further calculations, the area is 720 km^2, the value of specific surface runoff is 8.5 $l/s.km^2$ and specific baseflow is 3.5 $l/s.km^2$ for the aquifers of the Shashemene sub-sheet. The assessed water resources of the Shashemene area are shown in table 7-7. There are good water resources to be used for irrigation, as well as for drinking water supply of people living within the area.

The total water resources of the area have been assessed to be 193 Mm^3/year. The surface water of rivers flowing from the eastern escarpment should be primarily used for irrigation; construction of irrigation dams on the intermittent rivers of the eastern escarpment can support agricultural production. The irrigation plans, including assessment of irrigation potential and environmental impacts, are discussed in detail by Halcrow (2008) for the Rift Valley Lakes basin.

Table 7-7. *Assessment of water resources of the Sashemene area.*

	Input	**Area [km^2]**	**Resources total**	**Remark**
Precipitation	1,300 mm	720	720 Mm^3/year	
Total water resources – map	8.5 $l/s.km^2$	720	193 Mm^3/year	21 % rainfall
Renewable groundwater resources aquifers	3.5 $l/s.km^2$	720	79 Mm^3/year	8 % rainfall

The river gauge measurements show that nearly 21 % of precipitation is drained as total runoff from the area and about 8 % of precipitation infiltrates and appears as baseflow. There are good groundwater resources to be used for the supply of drinking water to people living within the area; however treatment of water (defluoridation) is necessary because of the high fluoride content in the groundwater in the western part of the sub-sheet. There is also the potential to use groundwater of the area to support irrigation. The total volume of renewable groundwater resources of active aquifers in the area has been assessed to be 80 Mm3/year.

Most of the people within the area live in Shashemene town and in small towns and villages along main roads in the western part of the sub-sheet. These people are supplied from drilled and dug wells and cold springs. Additional to further development of protected springs and dug wells, water supply based on drilled wells represents the most sanitary secure water and should be applied for Shashemene and small towns as well as for rural inhabitants.

To select appropriate areas, data from regional as well as detailed surveys have been evaluated and a strategy was chosen which consists in siting the hydrogeological wells for supplying the population on the following basis:

1. Groundwater accumulated in the volcano-clastic and volcano-sedimentary materials in the western part of the sub-sheet contains increased concentrations of TDS as well as fluoride, which overreach standards for potable water.
2. Volcanic rocks like basalts and ignimbrites in the eastern part of the sub-sheet contain groundwater, the quality of which mostly corresponds with the standards for potable water.
3. The yields of the wells which penetrate volcanic rocks (fissured and mixture aquifers) fluctuate between 2 and 10 l/s, and they are sufficient for the supply of as many as 8,000 to 40,000 inhabitants, the consumption of per person being 20 l/day.

The strategy for the layout of the wells, resulting from the above-mentioned presumptions, is as follows:

1. To prefer the location of the boreholes on the outcrops of dark rocks (basalt, trachyte, rhyolite and ignimbrite).
2. If there are only light-colour volcanic-sedimentary rocks, to perform a geophysical survey to determinate the boundary line between these rocks and the underlying volcanic rocks.
3. To locate the open section of the well in the fissured part of the volcanic rocks.
4. To obdurate the overlying volcanic-sedimentary rocks in the boreholes by cement seal to avoid fast penetration of the water from these rocks along the stem of the well. This strategy as also the most important particularly in the north-western area where Wendo Koshe pumices fall and yellowish phreatomagmatic tuffs cover a large area of the rift floor.

Table 7-8. *Proposed sites for drilling of water supply wells.*

Site No.	Site	Coordinates (UTM)			Site tested by geophysical investigation	Aquifer / lithology
		X	Y	Elevation m a.s.l.		
1	Sole	462384	792602	2160	VES, EP	Mixed aquifers, ignimbrite covered by Wendo Koshe pumice fall and yellow tuffs
2	Faji	465783	790674	2340	VES, EP	Mixed aquifers, ignimbrite
3	Bomba next to DW	454032	790987	1950	VES, EP	Mixed aquifers, ignimbrite covered by Wendo Koshe pumice fall
4	Jigesa	464114	796448	2120	VES, EP	Mixed aquifers, ignimbrite covered by Wendo Koshe pumice fall and yellow tuffs
5	Wetera	466482	799091	2120	VES, EP	Mixed aquifers, ignimbrite covered by Wendo Koshe pumice fall and yellow tuffs
	Wendo Genet escarpment	(general)		1900	VES, EP	Mixed aquifers, ignimbrite

*Remark: VES–Vertical Electrical Sounding, EP-electric profiling *) not located on the map – general drilling site*

The chosen strategy should be applied in the sedimentary rocks around Lake Cheleleka, which corresponds to the situation developed on the eastern shore of Lake Hawasa, where ignimbrite and basalt ridges can be found within lacustrine sediments and in the northeast where the surface is covered by Wendo Koshe pumice fall and yellow tuffs. It is assumed that a borehole drilled in accordance with the above proposal will have a sufficient yield and that the water will not contain an excessive concentration of fluoride. Other areas for drilling of water wells are in the fissured and mixed aquifers of the Shashemene sub-sheet. Table 7-8 documents the location of the sites proposed for drilling of wells. These sites are shown on the hydrogeological map but the exact well setting should be checked by individual geophysical investigations prior to drilling. These drilled wells are proposed in the western part of the area to support drinking water supply for people working in dynamically developing state farms.

The proposed depth of boreholes should be designed based on the optimum cost and yield of individual wells depending on the local situation in the aquifer. During the final siting of each well it is necessary to consider that the final depth of the proposed wells is governed by the level of groundwater which is given by the drainage level (surface water level in the river or lake) and the surface level of the site selected for well drilling. The drainage level (groundwater level) for each specific site should be derived from the nearby surface water level in the river and should be confronted with the site specific surface level of the drilling site and wells drilled before in the vicinity of the proposed well. Other technical, quantitative and qualitative data for proposed drilled wells are shown in table 7-9.

Table 7-9. *Technical, quantitative and qualitative data for proposed drilled wells.*

Site No.	Site	Depth (m)	Drill diameter (mm)	Drill method	SWL (m)	Yield (l/s)	TDS (mg/l)	Temp. (C^o)
1	Sole	250	356 / 305	DTH	80	2.5	500	15
2	Faji	250	356 / 305	DTH	80	3	500	15
3	Bomba next to DW	250	356 / 305	DTH	100	3	500	15
4	Jigesa	250	356 / 305	DTH	100	4	500	15
5	Wetera	250	356 / 305	DTH	100	2.5	500	15
	Wondo Genet area	200	356 / 305	DTH	50		500	17

The most difficult question will be supply to rural areas with a widely spread population. This should be done from local centres where water wells will be drilled and connected to places of water use with relatively long distribution pipes. The effectiveness and cost of water supply systems for the rural population should be studied as a site specific problem in the future.

The potential of groundwater resources is not sufficient for the current needs of people living in these areas. There is a chance to use the groundwater of the eastern highlands and escarpment for water supplies of the central part of the rift valley, particularly where there is a problem with water quantity and quality (high TDS and fluoride content).

Deeper wells currently represent a safe type of water supply; however, they have to be protected against pollution from local sources like human and animal waste (sources of pathogens and nitrates) as well as from potential industry (tanneries, textile industry, flower plantations, etc.). The minimum required distance of water supply wells and potential pollution sources should be maintained during water resource development in towns and villages. The same level of interest should also be applied to the development and protection of groundwater resources for rural communities. It should be necessary to start with relatively concentrated communities where the feasibility and impact of developed schemes will be most significant.

In addition to priority in development of groundwater for safe drinking water supply, it should be possible to select the most fertile soil nearby human settlements and adequate water resources to be developed for irrigation based on groundwater to increase the stability of food supply in prolonged periods of drought. Development and protection of the water resources of the area and the environment as a whole have a principal importance for the development of the infrastructure with subsequent impacts upon the eradication of poverty (development of irrigated agriculture, maintaining livestock during drought).

8. GEOLOGICAL HAZARDS

8.1. Endogenous hazards

8.1.1. SEISMIC AND TECTONIC HAZARDS

SEISMICITY OF SOUTHERN ETHIOPIA

Southern Ethiopia reveals seismic activity, which combines several types of earthquakes. Shallow seismic swarms are connected with the movement of magma and magma-derived fluids (vapour, CO_2, etc.). The swarms consist of many thousands of weak to moderate earthquakes with magnitudes of less than 5. Another type of earthquake accompanies direct volcanic eruptions as observed several times in history (Gouin, 1979). Strong tectonic earthquakes are believed to be connected with normal movements on faults parallel to the rift valley. However, alternative models are possible as well. Young tectonic movements of various orientations, even non-parallel to the rift, have been observed on the surface. Historical earthquakes are poorly located and cannot be assigned to known faults. The focal mechanisms of historical earthquakes are completely unknown and their hypocentral depths are undetermined too. The seismic exploration of this area is inadequate to define the source zones for seismic hazard assessment. This means that a strong earthquake should be considered possible anywhere in southern Ethiopia. For this reason, the scope of the sub-chapter was extended from the sub-sheet area to the whole of southern Ethiopia.

There are two reported earthquakes with epicentres fitting to the area of the Shashemene sub-sheet. The earthquake from September 6th 1944 is likely to have taken place in the south-western corner of the sub-sheet, but the location and even the occurrence of this event is very uncertain. There was, however, another earthquake (magnitude 5.1) on December 2nd 1983 most likely in the area between the Lake Cheleleka basin and the Wendo Genet scarp to the south of Wendo Genet. Due to the poor coverage of seismic stations in the area, not even the latest event is localized with a precision exceeding ± 50 km. For this reason, we have not plotted the epicentres of these earthquakes on the map at the scale of 1 : 50,000.

LOCAL AMPLIFICATION OF SEISMIC WAVES

Generally speaking, localities with thick sedimentary layers (characterized by low S-wave velocities) reveal the strongest amplification of seismic motion. These areas are shown on the map. However, many other factors are also important, namely the topography of the surface and of the bottom of the sedimentary layers, types of propagating seismic waves, their azimuth and angle of incidence, frequencies close to eigen-frequencies of the structure model, depths of earthquake hypocenters, propagation effects along the wave path between the source and the site, etc. For this reason, the areas shown on the map should be considered only as the first approximation of the most hazardous areas.

FISSURES

Ground cracks have not been documented in the area of the Shashemene sub-sheet. Nearly 5 km long N-S trending crack is developed to the south of Lake Shalla, more than 7 km north of the Shashemene sub-sheet. This prominent fissure might potentially expand southward to the area closer to Shashemene in the future.

8.1.2. VOLCANIC HAZARDS

The Shashemene sub-sheet area is located to the east of the active volcanoes of the Corbetti volcanic system (Wendo Koshe and Chebi – Biggs et al. 2011; Rapprich et al. 2013). Such a position is vulnerable in the zone of predominating western winds.

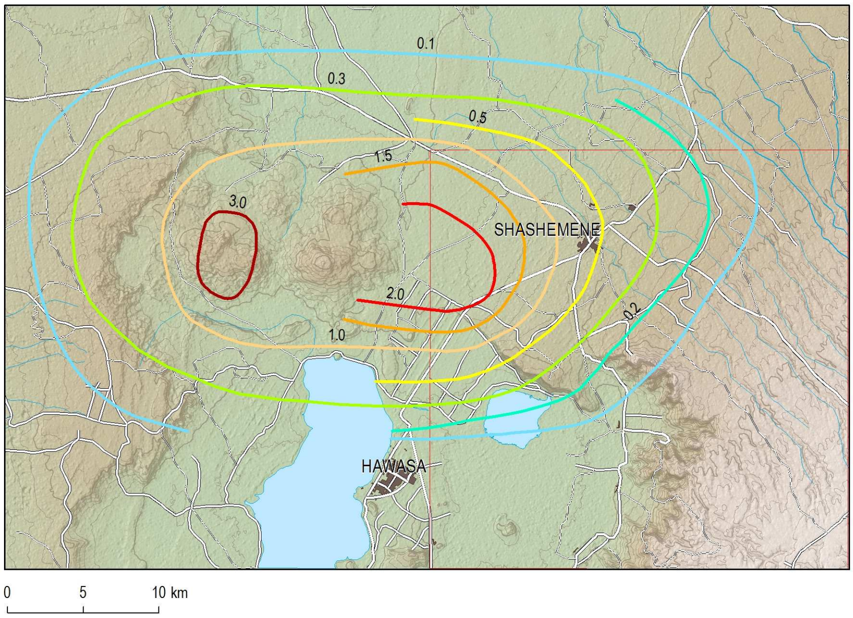

Figure 8-1. *Isopach (in m) scheme of the young Wendo Koshe pumice fall deposit (Shashemene sub-sheet in red).*

EXPLOSIVE ERUPTIONS

According to the geological record, explosive eruptions in the area of the Corbetti Caldera do not happen as frequently as effusive eruptions during the Holocene. The main polygenetic explosive vent remains Wendo Koshe in the central part of the Corbetti Caldera on the Hawasa sub-sheet. The time since the last explosive eruption and the frequency of explosive eruptions are not known. Should a new Plinian style eruption take place on the Wendo Koshe Volcano, even Shashemen would be covered by a 0.5 m thick deposit of pumice preventing cattle from feeding and also covering sources of water. An isopach map of the thickness of pumice fall from the last explosive eruption of the Wendo Koshe Volcano is shown in figure 8-1.

MAFIC MONOGENETIC VOLCANISM

Monogenetic cones of the Hawasa basaltic belt were presumed to be extinct. Recent studies have shown, that mafic monogenetic volcanism in this area occurred repeatedly in various episodes and could therefore repeat again. Small volume basaltic monogenetic eruptions would affect a limited area (several square kilometres), but would represent a serious risk if they happened within the densely populated area (Town Hawasa). We have also to take into account two possible scenarios for such an eruption. On the basaltic ridge, a dry Strombolian style eruption could be expected, but if such an eruption took place in the swampy area around Lake Cheleleka, the water would cause more intense fragmentation and the eruption would more likely be of Surtseyan style, emitting more dust to the atmosphere and affecting a larger area windward.

8.2. *Exogenous hazards*

The eastern part of the Shashemene sub-sheet area is characterized by expressive escarpments. Rapid expansion of settlements and the associated needs for agriculture and other human activities have changed the land use abruptly over the last tens of years. By consequence, exogenous geological hazards are becoming an ever more serious problem to the people living in the area. The area is strongly affected by various types of erosion related to loss of land and creation of fissures on the surface of the rift floor.

8.2.1. EROSION-RELATED HAZARDS

GULLY AND RILL EROSION

Gully and rill erosion is associated with ephemeral streams and occurs in the eastern part of the sub-sheet with gentle slopes upon Corbetti ignimbrites overlain by phreatomagmatic tuffs. The erosion cuts through the lateritized and loose non-welded pyroclostic deposits being stopped on the top of the welded facies of the Corbetti ignimbrite. Down in the lowlands, the streams decelerate and most of the water is infiltrated into non-welded, poorly consolidated pyroclastic deposits. For that reason, gully erosion is not developed in the western part of the sub-sheet.

The gullies are several metres deep at most and have no tendency to propagate in depth or in width.

SHEET EROSION

Sheet erosion does not significantly affect the area of the Shashemene sub-sheet. Despite the fact, we must not exclude the future possibility of expansion of sheet erosion in the case of improper land use and agriculture not respecting the lithological and geomorphological factors influencing the vulnerability of the landscape.

8.2.2. SLOPE DEFORMATION HAZARDS

We documented two areas with slope deformation hazards on the map. The first is located southwest of Shashemene on the steep fault scarp of Weransa Ridge (Shalo area) and the second is in the Wendo Genet mountains area. Both areas are characterized by different types of movement. The Shalo scarp is typical for rock fall and toppling and Wendo Genet is characterised by landslides or complex slope deformations including small earth flows.

ROCK FALL AND TOPPLING

The areas endangered by rock fall and toppling are located especially on the southern slopes of Weransa Ridge. The scarp is 100–300 m high and about 4 km long. The rock walls rise nearly vertically, with talus of debris cones and old rock-fall deposits on the foothills (figure 8-2). The thickness of deposits could exceed 50 m. Large blocks (figures 8-3 and 8-5) and debris deposits (figures 8-2 and 8-4) from extensive rock falls are documented over the entire length of Weransa Ridge. Slopes are formed by Hawasa crystal-rich rhyolite and in the western part by Corbetti blocky rhyolitic ignimbrite. Both lithologies are characterized by columnar jointing which predisposes the rocks to decomposition and slope movement (figure 8-4.). The slope is of tectonic origin and columnar jointing results from cooling contraction of volcanic rocks and welded pyroclastic deposits (ignimbrites). The main rock-fall triggering factors for are heavy rains and seismic events.

Recommendation: The dirt road along the foot-hill is at permanent risk of rock-falls. Therefore, we recommend shifting the road away from the slope. If any buildings were constructed with an aim of balneological use of the Shalo thermal spring, technical protection of the site would be necessary.

Remediation of the site is possible using dynamic barrier systems at the foothill of the slope (Geobrugg AG, Maccaferri S.p.a.). More detailed site investigation is necessary before any work is performed.

Figure 8-2. *Rock-fall deposits at the foothill of the Weransa Ridge slope. Photo P. Kycl.*

Figure 8-3. *Some collapsed blocks have volumes exceeding 20 m^3. Photo P. Kycl.*

Figure 8-4. *Columnar jointing of rhyolite with the collapsed part of the massif. Photo P. Kycl.*

Figure 8-5. *Collapsed block on the foothill road. Photo P. Kycl.*

LANDSLIDES

Landslide occurrences were mapped from remote sensing data and field work. Published studies from the area were also used for recognition of zones prone to slope deformation hazards. The large extent of ancient landslides became clear from the results of the field work (figure 8-6). Especially in the middle part of Wesha River, on the slopes to the east of the Wendo Genet hot springs area (figure 8-7). Concerning to geology, Wendo genet area is created by Corbetti rhyolitic ignimbrites those surface is deeply lateritized. According to the mapping methodology, only landslides more than 100 m in length were mapped. Old landslides of such dimensions cover the slopes around Gulbicha, Dabicho Ridge and Mt. Abaro (2,580 m a.s.l.). Moreover a total of 63 small landslide indications were identified and mapped. The area of the Shashemene sub-sheet includes 53 of them (figure 8-8).

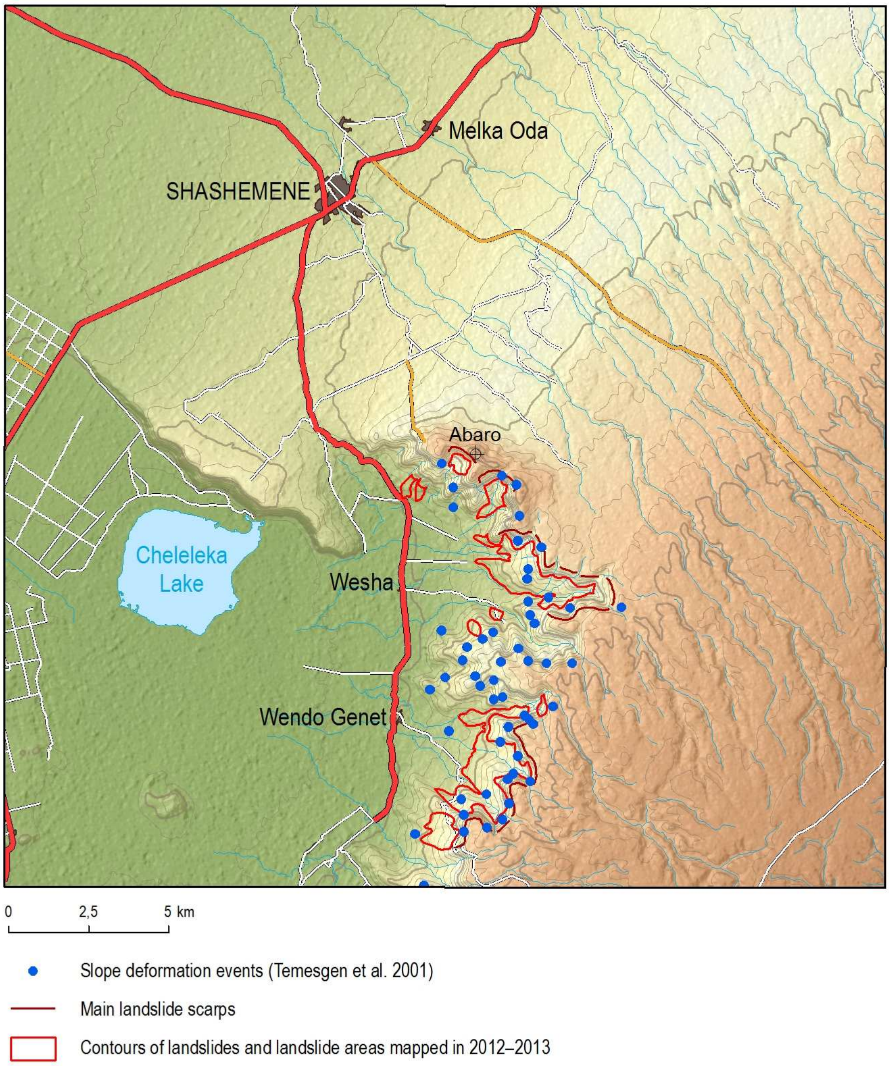

Figure 8-6. *Scheme of mapped landslides and published slope-deformation events.*

Figure 8-7. *An ancient landslide covers a large area on slopes east of the hot springs. Photo P. Kycl.*

Figure 8-8. *Landslide deposits – blocks of ignimbrites in a silty matrix. Photo P. Kycl.*

8.3. Hydrological and hydrogeological hazards

Water-related hazards are mainly limited to the following phenomena: heavy rainfall causing erosion and floods, increasing depth of rainfall over several consecutive years accompanied by a rise in water levels of Lake Cheleleka and floodings in its vicinity.

8.3.1. INUNDATION

Inundation does not represent a serious problem in the area of the Shashemene sub-sheet as the fluvial system is not very dense and drains small catchments. However, heavy rainfall may cause flash floods in many ephemeral rivers systems and erosional valleys.

Water level fluctuation of Lake Cheleleka may represent a serious natural hazard for the scarce population scattered in the swamps around the lake. The rise in the water level of Lake Cheleleka is caused by sediment aggradation in the basin. Siltation of Lake Cheleleka was documented by Tadesse and Zenaw (2003). The surface area of Lake Cheleleka was about 12 km^2 in 1972, but currently it is completely filled by sediment transported from the eastern highlands due to deforestation in this area.

8.3.2. FLUORIDE

The problem with the **high fluoride content** in the water of the Hawasa and Shashemene area is very well known and is described in many studies. The fluoride concentration frequently exceeds 3 mg/l which will cause mild fluorosis (mottling of teeth). Higher fluoride concentrations in drinking water cause both dental and skeletal fluorosis resulting in serious public health problems. The treatment of fluoride in groundwater, if viable, could resolve a number of pressing water supply problems in the area.

Fluoride concentrations are particularly high in areas with an occurrence of thermal waters or near areas of recent volcanism (e.g., around the Corbetti Caldera). There is a direct correlation between silicic volcanic rocks such as obsidian and pumice and high concentrations of fluoride in groundwater. It is considered that leaching of water soluble Na-fluorides coating pyroclasts is the most likely source of fluoride. The rhyolitic rocks are extremely poor in phosphorus which would lead to fixing of the fluorine in apatite and they lack calcium which would react with fluorine producing non-leachable calcium fluoride. The interaction of the rhyolitic pyroclastic rocks with a large effective surface and percolating groundwater and carbon dioxide at high pH causes the release of fluoride into the groundwater. It is suggested (Rango et al. 2009) that the fluoride concentration in groundwater is inversely related to the concentration of Ca. This permits free mobility of the fluoride ion into groundwater at lower Ca content. This effect (Ca deficiency) is magnified where cation exchange takes place within the sediments (fluvio-lacustrine, volcano-lacustrine) causing the removal of ions from the solution (mainly Ca^{2+}) and replacement with Na^+ ions from the clay. Such hydrogeochemical processes are responsible for the evolution of Ca (Mg)–HCO_3 types of water of the highlands and the escarpment area to Na–HCO_3 types of groundwater (including the thermal water of the rift floor).

Thermal water tends to have a higher fluoride content than cold water as the water temperatures allow greater dissolution of fluoride. This probably explains the preponderance of high fluoride in waters around Hawasa town. It was also mentioned that closed terminal lakes attain high fluoride, salinity and alkalinity as a result of evaporation and the groundwater flux that comes through the acidic rocks. High concentrations can also be observed in the north-eastern area of the Bilate River, the surroundings of Lake Hawasa as well as in the lake itself.

It was shown by Tadesse and Zenaw (2003) and by JICA (2012) that fluoride contents decrease with increasing depth of the water source (testing wells). This confirms that the main source of fluoride is related to infiltration of rain water through young deposits of silicic volcanic activity. The concentration of course can be enhanced in geothermal systems. The same is also valid for the concentration of chlorides as well as nitrates. Tadesse and Zenaw (2003) noted that the decrease of fluoride with depth in the area indicates that the shallower lacustrine aquifer has a high concentration of fluoride (figure 8-9).

UNDP (1971) listed the content of fluoride of Chabbi obsidian of 2,500, pumice 440, obsidian 400, rhyolite 300, and ignimbrite 410 ppm. Samples of rocks were collected from the tuff and pumice of the Shashemene area during the field trip of 2012. Partial results of the chemical composition of samples analysed in the laboratory of CGS are shown in table 8-1 as well as the composition of leachate analysed in the laboratory of AQUATEST.

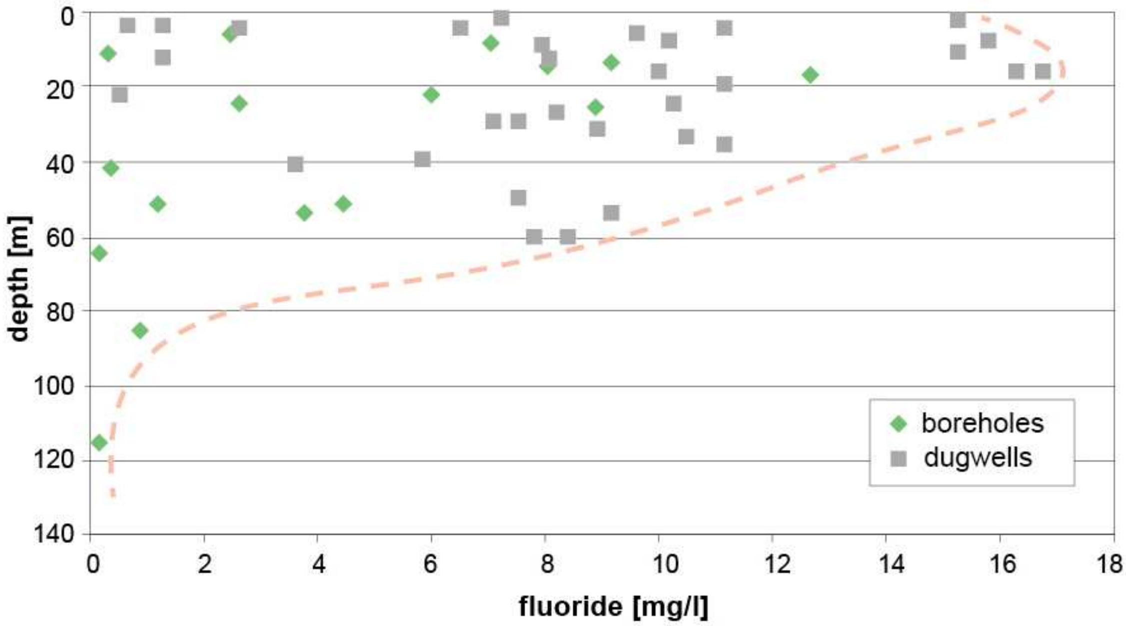

Figure 8-9. *High content of fluoride is caused by its leaching from silicic pyroclastic deposits. A decrease in fluoride content in groundwater with increasing depth is most likely the effect of depletion of older pyroclastic deposits and lacustrine sediments due to higher age and longer leaching of fluoride in the past.*

Table 8-1. *Chemical composition of rock samples in wt. % and chemical composition of leachate from these rocks in mg/l. See Annex 1 for details of sample location and complete geochemistry.*

Sample	**Rock sample composition**				**Leachate composition**			
	CaO	**Na_2O**	**K_2O**	**F**	**Ca**	**Na**	**K**	**F**
HSRV009	1.18	3.52	4.76	0.209	2.5	32.8	5.28	4.16
HSRVR069D	0.58	4.13	4.19	0.199	4.2	6.42	0.74	1.37
HSRVR069C	0.30	4.05	4.17	0.192	1.1	9.39	0.66	1.89
Sd007	0.28	4.96	4.39	0.218	5.4	4.25	< 0.5	0.74

A number of fluoride removal methods are practiced in basic water treatment plant design. The method of adding gypsum to the artificial sand-pack filter of a borehole and mixing of hot water with cold water was successfully tested in fluoride rich groundwater in Mexico (Carrillo-Rivera, 2002).

8.4. Anthropogenic hazards

Waste dumps in the area of the Shashemene sub-sheet represent a serious hazard to human health. The mixed communal waste containing spent cans and bottles from paints and toxic chemicals is deposited in abandoned sandpits without any insulation. The highly permeable rocks enable the migration of toxic substances from the waste dumps towards sources of drinking water. Such deposits are located close to the town of Shashemene; one is on the southern edge of the town (figure 8-10) and the second is some 4 km to the west of the town.

Table 8-10. *Waste dump in an abandoned sandpit in permeable pyroclasti deposits. Photo V. Rapprich.*

REFERENCES

ABEBE (1984): Geological and petrological study of Tulu Moye and Gedemsa Geothermal Project. Unpublished report. Pisa, Italy.

ACOCELLA V. (2010): Coupling volcanism and tectonics along divergent plate boundaries: Collapsed rifts from central Afar, Ethiopia. Geological Society of America Bulletin, 9–10: 1717–1728.

AGOSTINI A., BONINI M., CORTI G., SANI F., MANETTI P. (2011): Distribution of Quaternary deformation in the central Main Ethiopian Rift, East Africa. Tectonics 30(4).

ASTATKE K., ŠÍMA J. (2012): Hydrogeological and hydrochemical maps of Asela NB 37-3. Explanatory notes. Aquatest a.s., Praha, Czech Republic.

BALOGH K. (1985): K/Ar Dating of Neogene Volcanic Activity in Hungary: Experimental Technique, Experiences and Methods of Chronologic Studies. ATOMKI Rep., D/1: 277–288.

BASALFEW Z. (ed., 2012): Geological map 1 : 250 000, Hoseina sheet with explanatory note. Geological Survey of Ethiopia.

BIGGS J., BASTOW I.D., KEIR D., LEWI E. (2011): Pulses of deformation reveal frequently recurring shallow magmatic activity beneath the Main Ethiopian Rift. Geochemistry, Geophysics, Geosystems 12: Q0AB10.

BILLI P., DRAMIS F. (2003): Geomorphological investigation on gully erosion in the Rift Valley and the northern highlands of Ethiopia. Catena 50.

BONINI M., CORTI G., INNOCENTI F., MANETTI P., MAZZARINI F., ABEBE T., PÉCSKAY Z. (2005): Evolution of the Main Ethiopian Rift in the frame of Afar and Kenya rifts propagation. Tectonics 24: TC1007.

BOYNTON W.V. (1984): Geochemistry of the rare earth elements: meteorite studies. – In: HENDERSON, P. (ed.), Rare earth element geochemistry. Elsevier: 63–114.

CARNICELLI S., BENVENUTI M., FERRARI G., SAGRI M. (2009): Dynamics and driving factors of late Holocene gullying in the Main Ethiopian Rift (MER). Geomorphology, 103: 541–554.

CARRILLO-RIVERA J.J. (ed. 2002): Use of abstraction regime and knowledge of hydrogeological condition to control high-flouride concentration in abstracted groundwater: San Luis Potosí basin, Mexico. Journal of Hydrogeology 261: 24–47.

DI PAOLA G.M. (1972): The Ethiopian Rift Valley (between 7° 00′ and 8° 40′ lat. north). Bull. Volcanol. 36: 517–560.

DI PAOLA G.M. (1976): Geological, Geothermal Report on Central Part of the Main Ethiopian Rift Valley. Geological Survey of Ethiopia, Addis Ababa, Ethiopia.

EBINGER C. (2005): Continental break-up: The East African perspective. Astronomy & Geophysics, 46: 216–221.

FAURE G., MENSING T.M. (2005): Isotopes: principles and applications. John Wiley & Sons Inc.

GEORGE R., ROGERS N. (2002): Plume dynamics beneath the African plate inferred from the geochemistry of the Tertiary basalts of southern Ethiopia. Contributions to Mineralogy and Petrology, 144: 286–304.

GOUIN P. (1979): Earthquake history of Ethiopia and the Horn of Africa. Ottawa, Ont., IDRC, 259 p.

HALCROW ind. (2008): Rift Valley Lakes Basin Integrated Resources Development Master Plan Study Project, Draft Phase 2 Report Part II Prefeasibility Studies, Halcrow Group Limited and Generation Integrated Rural Development (GIRD) consultants. Unpublished report. Addis Ababa.

HAYWARD, N.J., EBINGER, C.J. (1996): Variations in the along-axis segmentation of the Afar Rift system. Tectonics, 15: 244–257.

JANOUŠEK V., FARROW C.M., ERBAN V. (2006): Interpretation of Whole-rock Geochemical Data in Igneous Geochemistry: Introducing Geochemical Data Toolkit (GCDkit). J. Petrol. 47, 1255–1259.

JICA (2012): The Study on Groundwater Resources Assessment in the Rift Valley Lakes Basin in the Federal Democratic Republic of Ethiopia, Japan International Cooperation Agency (JICA), Kokusai Kogyo Co., Ltd., Ministry of Water and Energy (MoWE), The Federal Democratic Republic of Ethiopia. Final Report (Main Report).

KAZMIN V. (1972): Geological map of Ethiopia, 1 : 2 000 000. UN, MME.

KAZMIN V., SEIFE M. BERHE (1978): Geological map of Nazreth sheet, Scale 1:250,000. Geological Survey of Ethiopia, Addis Ababa, Ethiopia.

KAZMIN V., SEIFE M. BERHE, WALSH J. (1981): Geological map of the Ethiopian Rift 1 : 500 000. Unpublished EIGS.

KEFALE T., ŠÍMA J. (2013): Hydrogeological and hydrochemical maps of Hosaina NB 37-2. Explanatory notes. Aquatest a.s., Praha, Czech Republic.

LE BAS M.J., LE MAITRE R.W., STRECKEISEN A., ZANETTIN B. (1986): A chemical Classification of volcanic rocks based on the total alkali-silica diagram. J. Petrol. 27: 745–750.

MCARTHUR J.M., HOWARTH R.J., BAILEY T.R. (2001): Strontium isotope stratigraphy: LOWESS version 3: best fit to the marine Sr-isotope curve for 0–509 Ma and accompanying look-up table for deriving numerical age. The Journal of Geology, 109: 155–170.

MENGESHA T., TADIWOS C., WORKINEH H. (1996): Geological map of Ethiopia 1 : 2 000 000 with Explanatory Note, second edition. Geological Survey of Ethiopia.

MOGES A., HOLDEN M.N. (2008): Estimating the rate consequences of gully development, a case study of Umbulo catchment in southern Ethiopia. Land Degrad. Develop. 19.

MoWR (2002): Negarit Gazeta No. 12/1990 and The Guidelines of Ministry of Water Resources.

ODIN G.S. (1982): Numerical Dating in Stratigraphy. John Wiley and Sons, New York, pp 1–1040.

PEARCE J.A. (1996): A user's guide to basalt discrimination diagrams. – In: WYMAN, D.A. (ed.), Trace element geochemistry of volcanic rocks: Applications for massive sulphide exploration. Geol. Assoc. Canada, short course notes 12: 79–113.

RANGO T., BIANCHINI G., BECCALUVA L., AYENEW T., COLOMBANI N. (2009): Hydro-geochemical study in the Main Ethiopian Rift: new insights to the source and enrichment mechanism of fluoride. Environmental Geology, 58: 109–118.

RAPPRICH V., ČÍŽEK D., DANIEL K., FIRDAWOK L., HABTAMU B., HROCH T., KOPAČKOVÁ V., MÁLEK J., MALÍK J., MIŠUREC J., ORGOŇ A., ŠEBESTA J., ŠÍMA J., TSIGEHANA T., VERNER K., YEWUBINESH B. (2013): Explanation Booklet to the Set of Geoscience maps of Ethiopia at scale 1 : 50,000, subsheet 0738-C4 Hawasa. Czech Geological Survey/Aquatest/Geological Survey of Ethiopia, Praha/Addis Ababa, Czech Republic/Ethiopia.

STEIGER R.H., JÄGER E. (1977): Subcommission on Geochronology: convention on the use of decay constants in geo- and cosmochronology. Earth and Planetary Science Letters, 36: 359–362.

STEWART K., ROGERS N. (1996): Mantle plume and lithosphere contributions to basalts from southern Ethiopia. Earth and Planetary Science Letters, 139: 195–211.

TADESSE D., ZENAW T. (2003): Hydrology and Engineering Geology of Awasa Lake Catchment, Geological survey of Ethiopia, 1–67 + 2 maps.

TEMESGEN, B., MOHAMMED, M .U., KORME T. (2001): Natural Hazard Assessment Using GIS and Remote Sensing Methods, with Particular Reference to the Landslides in the Wondogenet Area, Ethiopia. Phys. Chem. Earth (C), Vol. 26, No. 9, pp. 665–615.

TEMESGEN B., UMER M., ASRAT A. (1999). Landslide hazard on the Dabicho, Wondo Genet area: the case of June 18, 1996 event. SENET: Ethiop. J. Sci., 22 (l):127–140.

TESFAYE C. (1982): Hydrogeology of the lakes region, Ethiopia, Ministry of Mines and Energy Ethiopian Institute of Geological Surveys. Addis Ababa.

TESFAYE C. (1993): Hydrogeology of Ethiopia and Water Resources Development. MS EIGS, Ministry of Mines and energy, Addis Ababa.

UNDP (1971): Ethiopia: Investigation of Geothermal Resources for Power Development (ETH 26). Geology, Geochemistry and Hydrology of Hot Springs of the Eastern African Rift System in Ethiopia.

VEIZER J., ALA D., AZMY K., BRUCKSCHEN P., BUHL D., BRUHN F., CARDEN G.A.F., DIENER A., EBNETH S., GODDERIS Y., JASPER T., KORTE C., PAWELLEK F., PODLAHA O.G., STRAUSS H. (1999): $^{87}Sr/^{86}Sr$, $\delta^{13}C$ and $\delta^{18}O$ evolution of Phanerozoic seawater. Chemical Geology, 161: 59–88.

WABCO (1990): Water Resources Development Master Plan for Ethiopia.

WOLDEGABRIEL G., ARONSON J.C., WALTER R.C., HART W.K. (1992): Geochronology and Distribution of Silicic Volcanic Rocks of Plio-Pleistocene Age from the Central Sector of the Main Ethiopian Rift. Quaternary International 13–14: 69–76.

WOLDEGABRIEL G., WALTER R.C., HART W.K., MERTZMAN S.A., ARONSON J.L. (1999): Temporal relations and geochemical feature of felsic volcanism in the central sector of the Main Ethiopian Rift. Acta Vulcanol. 11: 53–67.

WWDST (2003): Wabe Shabelle River Basin Integrated Development Master Plan Study. MoWR, Addis Ababa, Ethiopia.